Electrophysiological Characterization of the Rat Epithelial Na^+ Channel (rENaC) Expressed in MDCK Cells

Effects of Na^+ and Ca^{2+}

Toru Ishikawa,*‡§ Yoshinori Marunaka,*‡§ and Daniela Rotin*‡§

From the *Hospital for Sick Children, Division of Respiratory Research, Toronto, Ontario M5G 1X8, Canada; and the ‡Department of Biochemistry, and §Department of Paediatrics, University of Toronto, Toronto, Ontario, Canada

ABSTRACT The epithelial Na^+ channel (ENaC), composed of three subunits (α, β, and γ), is expressed in several epithelia and plays a critical role in salt and water balance and in the regulation of blood pressure. Little is known, however, about the electrophysiological properties of this cloned channel when expressed in epithelial cells. Using whole-cell and single channel current recording techniques, we have now characterized the rat αβγENaC (rENaC) stably transfected and expressed in Madin-Darby canine kidney (MDCK) cells. Under whole-cell patch-clamp configuration, the αβγrENaC-expressing MDCK cells exhibited greater whole cell Na^+ current at −143 mV (−1,466.2 ± 297.5 pA) than did untransfected cells (−47.6 ± 10.7 pA). This conductance was completely and reversibly inhibited by 10 μM amiloride, with a Ki of 20 nM at a membrane potential of −103 mV; the amiloride inhibition was slightly voltage dependent. Amiloride-sensitive whole-cell current of MDCK cells expressing αβ or αγ subunits alone was −115.2 ± 41.4 pA and −52.1 ± 24.5 pA at −143 mV, respectively, similar to the whole-cell Na^+ current of untransfected cells. Relaxation analysis of the amiloride-sensitive current after voltage steps suggested that the channels were activated by membrane hyperpolarization. Ion selectivity sequence of the Na^+ conductance was $Li^+ > Na^+ >> K^+ =$ *N*-methyl-D-glucamine$^+$ ($NMDG^+$). Using excised outside-out patches, amiloride-sensitive single channel conductance, likely responsible for the macroscopic Na^+ channel current, was found to be ~5 and 8 pS when Na^+ and Li^+ were used as a charge carrier, respectively. K^+ conductance through the channel was undetectable. The channel activity, defined as a product of the number of active channel (n) and open probability (P_o), was increased by membrane hyperpolarization. Both whole-cell Na^+ current and conductance were saturated with increased extracellular Na^+ concentrations, which likely resulted from saturation of the single channel conductance. The channel activity (nP_o) was significantly decreased when cytosolic Na^+ concentration was increased from 0 to 50 mM in inside-out patches. Whole-cell Na^+ conductance (with Li^+ as a charge carrier) was inhibited by the addition of ionomycin (1 μM) and Ca^{2+} (1 mM) to the bath. Dialysis of the cells with a pipette solution containing 1 μM Ca^{2+} caused a biphasic inhibition, with time constants of 1.7 ± 0.3 min ($n = 3$) and 128.4 ± 33.4 min ($n = 3$). An increase in cytosolic Ca^{2+} concentration from <1 nM to 1 μM was accompanied by a decrease in channel activity. Increasing cytosolic Ca^{2+} to 10 μM exhibited a pronounced inhibitory effect. Single channel conductance, however, was unchanged by increasing free Ca^{2+} concentrations from <1 nM to 10 μM. Collectively, these results provide the first characterization of rENaC heterologously expressed in a mammalian epithelial cell line, and provide evidence for channel regulation by cytosolic Na^+ and Ca^{2+}.

KEY WORDS: epithelial Na^+ channel • patch-clamp • Madin-Darby canine kidney cells • Na^+ • Ca^{2+}

INTRODUCTION

Amiloride-sensitive epithelial Na^+ channel(s) fulfills a variety of physiological roles in different Na^+-transporting epithelia such as those in the distal nephron, distal colon, lung epithelia, and duct cells of exocrine glands (Garty and Palmer, 1997). Previous electrophysiological studies show that these channels display functional heterogeneity in different tissues in terms of biophysical characteristics, including unitary conductance, kinetics, ion selectivity, and sensitivity to amiloride (Palmer, 1992). It is unclear whether this phenotypic heterogeneity reflects a corresponding genotypic diversity.

The first amiloride-sensitive epithelial Na^+ channel (ENaC)[1] was cloned from rat (rENaC) colon by functional expression cloning, and shown to be composed of three homologous subunits, α, β, and γ ENaC (Canessa et al., 1993, 1994*a*; Lingueglia et al., 1993, 1994). ENaC subunits have since been identified in different species, including human (hENaC) (McDonald et al., 1994, 1995; Voilley et al., 1994), *Xenopus* (xENaC) (Puoti et al., 1995), bovine (αbENaC) (Fuller et al., 1995), and chicken (αcENaC) (Goldstein et al., 1997). The cloned

Address correspondence to Dr. Toru Ishikawa, Division of Respiratory Research, Research Institute, The Hospital for Sick Children, 555 University Avenue, Toronto, Ontario, Canada M5G 1X8. Fax: 416-813-5771; E-mail: drotin@sickkids.on.ca

[1]*Abbreviations used in this paper:* ENaC, epithelial Na^+ channel; I-V, current–voltage; MDCK, Madin-Darby canine kidney; NMDG, *N*-methyl-D-glucamine.

J. Gen. Physiol. © The Rockefeller University Press • 0022-1295/98/06/825/22 $2.00
Volume 111 June 1998 825–846
http://www.jgp.org

ENaC subunits show structural and sequence similarities between these species; they all possess two transmembrane domains flanked by a large extracellular loop and two short NH_2 and COOH termini (Canessa et al., 1994*b*; Snyder et al., 1994; Renard et al., 1994).

ENaC has since attracted a particular attention for the following reasons: (*a*) this cloned channel expressed in *Xenopus* oocytes shares several common biophysical properties with those of the highly selective Na^+ channels that mediate Na^+ entry into distal segments of the kidney (reviewed in Garty and Palmer, 1997); (*b*) several heritable mutations in the genes encoding the ENaC subunits cause genetic disorders, including pseudohypoaldosteronism type I and Liddle's syndrome (Shimkets et al., 1994; Chang et al., 1996; Strautnieks et al. 1996); (*c*) inactivation of αENaC by targeted gene knock out in mice causes an early death due to defective lung fluid clearance at birth, demonstrating that this channel also plays a critical role in lung function (Hummler et al., 1996).

Despite the importance of the cloned ENaCs in epithelial cells, their functional aspects have been studied mainly by heterologous expression in nonepithelial cell systems such as *Xenopus* oocytes and planar lipid bilayer reconstitution (reviewed in Garty and Palmer, 1997). Single channel conductance of rENaC studied in planar lipid bilayers (13 pS) (Ismailov et al., 1996) is different from that observed in *Xenopus* oocytes (4–5 pS) (Canessa et al., 1994*a*), and the existence of a subconductive behavior of rENaC in planar lipid bilayers (Ismailov et al., 1996) has not been observed in patch records of rENaC expressed in *Xenopus* oocytes (Canessa et al., 1994*a*). Moreover, cAMP-dependent activation of ENaC was not observed in either *Xenopus* oocytes or in lipid bilayer systems (Awayda et al., 1996), in contrast to the stimulatory effects of cAMP on most amiloride-sensitive Na^+ channels in native tight epithelia, including mammalian collecting tubules and amphibian epithelia (reviewed in Garty and Palmer, 1997). The αβγrENaC transfected in NIH-3T3 fibroblasts, however, responded to cAMP (Stutts et al., 1995, 1997). Comparison of ENaC properties obtained in these systems raises the possibility that their biophysical characteristics and regulatory mechanism may depend upon the physical state of the membrane into which they are inserted, and on the cytosolic micro-environment, both heterogenous in different cell types.

Na^+ channel activity in native tight epithelia is regulated by various hormones such as aldosterone and vasopressin (reviewed in Rossier and Palmer, 1992; Garty and Palmer, 1997). In addition, it has been proposed that inorganic cations such as Na^+ and Ca^{2+} may also regulate channel activity. Previous studies have demonstrated that increasing luminal Na^+ concentration resulted in saturation of Na^+ entry in frog skin (Fuchs et al., 1977), toad urinary bladder (Palmer et al., 1980; Li et al., 1982), and rabbit descending colon (Thompson and Sellin, 1986; Turnheim et al., 1983). This saturation has been explained by the following mechanisms: (*a*) saturation of the single channel conductance by external Na^+ (Palmer and Frindt, 1986, 1988); (*b*) inhibition of Na^+ channels by extracellular Na^+ itself ("self-inhibition"); (*c*) inhibition of Na^+ channels due to changes in cytosolic composition such as Na^+ and Ca^{2+} ("feedback inhibition") (Chase, 1984; Garty and Lindemann, 1984; Palmer, 1985; Silver et al., 1993). Since all of the above studies using intact epithelia had several parameters changed simultaneously (e.g., membrane potential, intracellular pH, concentrations of Na^+ and Ca^{2+}), the detailed mechanisms by which intra- or extracellular Na^+ and/or Ca^{2+} regulate these channels remain unclear. Furthermore, the exact molecular identity of the channels studied in these native epithelia is not known.

Recently, Stutts et al. (1995) have demonstrated, using short circuit current measurements, that stable expression of rENaC in Madin-Darby canine kidney (MDCK) epithelial cells exhibited amiloride-sensitive transepithelial sodium currents, which could be stimulated by cAMP. Such a mammalian epithelial cell line stably expressing rENaC should allow electrophysiological and biochemical characterization of this molecularly known channel. To our knowledge, neither whole-cell nor single-channel currents via rENaC heterologously expressed in any mammalian epithelial cells have been extensively characterized. In the present paper, therefore, we provide a characterization of Na^+ conductance attributable to rENaC heterologously expressed in MDCK cells using patch-clamp techniques. We first used the whole-cell patch-clamp technique to characterize the biophysical properties of macroscopic currents from populations of rENaC channels in this heterologous expression system. We also performed single channel recording experiments to characterize the properties of the microscopic single channel conductance, which could be responsible for the macroscopic currents. We then studied the effects of Na^+ and Ca^{2+} on rENaC activity. In this report, we demonstrate that (*a*) the whole-cell Na^+ conductance attributable to rENaC activity saturates with increasing extracellular Na^+ concentration likely due to saturation of the single channel conductance, (*b*) single channel activity is inhibited by high cytosolic Na^+ concentrations, and (*c*) an increase in cytosolic Ca^{2+} has an inhibitory effect on rENaC expressed in MDCK cells.

METHODS

rENaC-expressing MDCK Cells

High resistance MDCK cells stably expressing αβγrENaC or αβrENaC were previously generated (and kindly provided by C.

Canessa and B. Rossier, University of Lausanne) by stably transfecting cells with αENaC in pLKneo (Hirt et al., 1992), which contains a dexamethasone-inducible promoter, together with β and γENaC cloned into a cytomegalovirus promoter-based vector and expressed constitutively (Stutts et al., 1995). Expression of the ENaC subunits was confirmed by immunoprecipitation of metabolically labeled channel using antibodies directed against each subunit (Stutts et al., 1995; Staub et al., 1997). MDCK cells stably expressing epitope-tagged αγrENaC were generated by transfecting FLAG-tagged (DYKDDDDK)γrENaC in pCEP4 (Invitrogen Corp., San Diego, CA), followed by triple HA-tagged (YPYDVPDY) αrENaC in pLKneo. Both tags were inserted just upstream of the STOP codon. Protein expression was verified by immunoblotting with antibodies to the tags. MDCK cells stably expressing αβγrENaC and αβrENaC were maintained in DMEM containing fetal bovine serum (FBS, 10%), penicillin (100 U/ml), streptomycin (100 μg/ml), G418 (300 μg/ml), and amiloride (10 μM) at 37°C in 5% CO_2-containing humidified air. Cells expressing αγrENaC were maintained as above, only with the addition of hygromycin (0.1 mg/ml). Wild-type MDCK cells were maintained in DMEM plus serum and antibiotics (without G418) as above. For patch-clamp experiments, cells were seeded at low density on a cover glass and patched 2–4 d after seeding. Only single cells were used for whole-cell patch-clamp experiments. rENaC-expressing MDCK cells were induced by adding 1 μM dexamethasone and 2 mM butyrate to the culture medium overnight, as described previously (Stutts et al., 1995).

Patch Clamp Analyses

Cells grown on cover glass were rinsed with an appropriate NaCl-rich bath solution (see below), and then transferred to a chamber mounted on a Leitz inverted microscope. Current recordings were made from MDCK cells using the standard whole-cell configuration of the patch-clamp technique (Hamill et al., 1981). The patch-clamp pipettes, which were pulled from glass capillaries (Dagan Corp., Minneapolis, MN) using a horizontal puller (P-97; Sutter Instruments Co., Novato, CA), had resistances of ~2–3 MΩ when filled with a standard Cs glutamate-rich solution.

An Axopatch-1D patch-clamp amplifier (Axon Instruments, Foster City, CA) was used to measure whole-cell and single channel currents. The reference electrode was a Ag/AgCl electrode that was connected to the bath via an agar bridge (10 mg/ml) filled with a NaCl-rich bathing solution. The amplifier was driven by pClamp software to allow the delivery of voltage-step protocols with concomitant digitization of the whole-cell current. The whole-cell currents were filtered through an internal four-pole Bessel filter at 1 kHz and sampled at 2 kHz.

Single-channel activity was recorded in cell-attached, inside-out, and outside-out patch configurations (Hamill et al., 1981) using an Axopatch-1D amplifier. Single-channel currents were filtered at 50–100 HZ with an internal four-pole Bessel filter, sampled at 1–2 kHz and stored directly on the computer's hard disk through the TL-1 DMA interface (Axon Instruments). Subsequent current analysis was performed using programs supplied with Axograph or pClamp software (Axon Instruments).

Current–voltage (I-V) relations were studied using 10-mV pulses, each of 400-ms duration, delivered at voltages ranging between −140 and +90 mV; voltage pulses were separated by 3–10 s, during which the cell potential was held at +40 or 0 mV. Steady state whole-cell currents were measured at 350 ms from the start of each voltage pulse. As an alternative to voltage steps, voltage ramps were applied. Typically, the command voltage was varied from −100 to +80 mV over a duration of 800 ms every 10 or 30 s. Reversal potentials were estimated by fitting linear regression lines at least to the three data points nearest to the zero current potential. Whole-cell conductances were calculated by fitting a linear regression to the data points between −53 and −103 mV. For kinetic analysis of the amiloride-sensitive whole-cell Na^+ currents, most relaxations were fitted with a single exponential using a least-squares method. To permit capacitive transients to subside, only data collected >10 ms after the potential change were used for the calculations. The amplitude of the relaxation was defined as the ratio of the steady state current (estimated as the asymptote of the exponential) to the initial current immediately after the potential change (estimated by extrapolation of the exponential to the time of the potential change). We have assumed that the relaxation amplitude, as defined here, equals the ratio of the fraction of channels open at the test potential to the fraction of channels open at the holding potential, and hence that it is proportional to the channel open probability.

To analyze titration curves for amiloride inhibition of the macroscopic Na^+ current (I_{Na}), the ratio I/I_0 measured in the presence (I) of amiloride to that in its absence (I_o), normalized to the value in the presence of 1 μM amiloride, was described by the following equation:

$$I/I_o = (1 - B) / (1 + (A/K_i)^{n'}) + B, \quad (1)$$

where K_i is the inhibitory constant of the blocker, A is the concentration of the blocker, n' is pseudo Hill coefficient, and B is a constant defined as the current remaining in the presence of maximal inhibition by amiloride.

In the case of a voltage-dependent block, $K_{i(V)}$ is the voltage-dependent inhibitory constant, which has been expressed by Woodhull (1973) as a Boltzmann relationship with respect to the voltage,

$$K_{i(V)} = K_{i(o)} \exp(z'FV/RT), \quad (2)$$

where $K_{i(o)}$ is the inhibitory constant at 0 mV, z' is a slope parameter, and F, V, R, and T have their conventional meanings. z' is equal to the product of the actual valence of the blocking ion z and the fraction of the membrane potential (or electrical distance) δ acting on the ion.

The K_m for external Na^+ was calculated from the whole-cell Na^+ current induced by varying the concentration (C) of Na^+ in the bath solution from 0 to 150 mM. The data were fitted to the Michaelis-Menten equation:

$$I = I_{max} [C/(K_m + C)], \quad (3)$$

where I_{max} is the maximal current and K_m is the half-activation constant using a nonlinear fit program.

The capacitance transient current in most experiments was compensated by using the Axopatch-1D amplifier. The cell capacitance was 33.0 ± 1.3 pF (n = 103). When constructing I-V plots, the steady state whole-cell current was measured at 350 ms after onset of the voltage pulse. The currents were not leak corrected. The series resistance (R_s) in these studies, which was 17.2 ± 0.6 MΩ (n = 103), was not compensated. The pipette potential was corrected for the liquid junction potentials between the pipette solution and the external solution, and between the external solution and the agar bridge, as described by Barry and Lynch (1990).

The compositions of the standard pipette and bath solution were as follows: the pipette solution (pH 7.4) contained (mM): 120 Cs-glutamate, 10 CsCl, 1 $MgCl_2$, 10 HEPES, and 1 EGTA. When the free Ca^{2+} concentrations of the pipette solution in whole-cell patch-clamp experiments were fixed at 10^{-6} M, 10 mM EGTA was used as a Ca^{2+} buffer. The free concentrations of Ca^{2+} were calculated from an equation that takes into account the concentrations of Mg^{2+}, Ca^{2+}, EGTA (96% purity), and pH (Oiki

and Okada, 1987), and the appropriate amount of $CaCl_2$ was added to the solution. The pH of the solution was adjusted with CsOH. The cells were initially immersed in bath solution (pH 7.4) containing (mM): 140 NaCl, 4.3 KCl, 1 $MgCl_2$, and 10 HEPES. After the formation of whole-cell configuration, the bath solution was changed to one containing (mM): 145 Na-glutamate, 1 $MgCl_2$, and 10 HEPES, pH 7.4. Relative permeabilities for various cations were determined using external solutions containing an equimolar amount of the glutamate salts of the test cation. The pH of the bath solutions was adjusted with LiOH, KOH, or NMDG-OH. When the free Ca^{2+} concentrations of the bath solution in inside-out patches were varied between 10^{-5} and $<10^{-9}$ M, 1 or 5 mM EGTA was used as a Ca^{2+} buffer. In these experiments, the bath solution was K- or NMDG-glutamate rich. The free concentrations of Ca^{2+} were calculated as described above.

All experiments were performed at room temperature (20–23°C). Bath solution changes were accomplished by gravity feed from reservoirs. The results were reported as means ± SEM of several independent experiments (n), where n refers to the number of cells patched, each from a different dish of cells. Statistical significance was evaluated using the two tailed paired and unpaired Student's t test. A value of $P < 0.05$ was considered significant.

RESULTS

Comparison of Whole-Cell Na^+ Conductance in Wild-Type and rENaC-transfected MDCK Cells

Previous studies have shown that MDCK cell membranes contain several types of K^+ and Cl^- channels (Lang et al., 1990). Thus, to isolate the Na^+ currents, the K^+ and Cl^- currents were minimized using Cs-glutamate-rich solution in the pipette, and by using glutamate as the major anion in bath solutions containing no K^+ ions. To compare whole-cell Na^+ conductance in untransfected vs. rENaC-expressing MDCK cells, we first measured the Na^+ current by changing the bath solution from a Na-glutamate-rich solution to a solution in which Na^+ was replaced by equimolar amounts of the impermeant $NMDG^+$ cation. Fig. 1 *A* shows that untransfected MDCK cells exhibited a small Na^+ conductance, with whole-cell Na^+ current amplitude of −27.0 ± 14.0 pA (n = 7) at −143 mV. A similar small conductance was also observed in these untransfected cells after overnight treatment with 1 μM dexamethasone and 2 mM butyrate (whole-cell Na^+ current amplitude at −143 mV was −47.6 ± 10.7 pA, n = 8). In contrast, rENaC-expressing MDCK cells exhibited a much greater Na^+ conductance, with whole-cell Na^+ current amplitude of −1,466.2 ± 297.5 pA (n = 14) at −143 mV (Fig. 1 *B, left*). These results indicate that rENaC-transfected MDCK cells express a functional Na^+ conductance at the plasma membrane.

Amiloride Sensitivity of the Na^+ Conductance

To determine if the Na^+ conductance observed in the rENaC-transfected MDCK cells is amiloride sensitive, we examined the effect of amiloride (10 μM) on the whole-cell Na^+ currents recorded from single cells expressing rENaC (Fig. 2). In the experiment shown in Fig. 2 *A*, we first measured the whole-cell I-V relation when the bath contained a Na-glutamate-rich solution, and then replaced the bath with a similar solution containing 10 μM amiloride. By subtracting the whole-cell records observed before the addition of the inhibitor

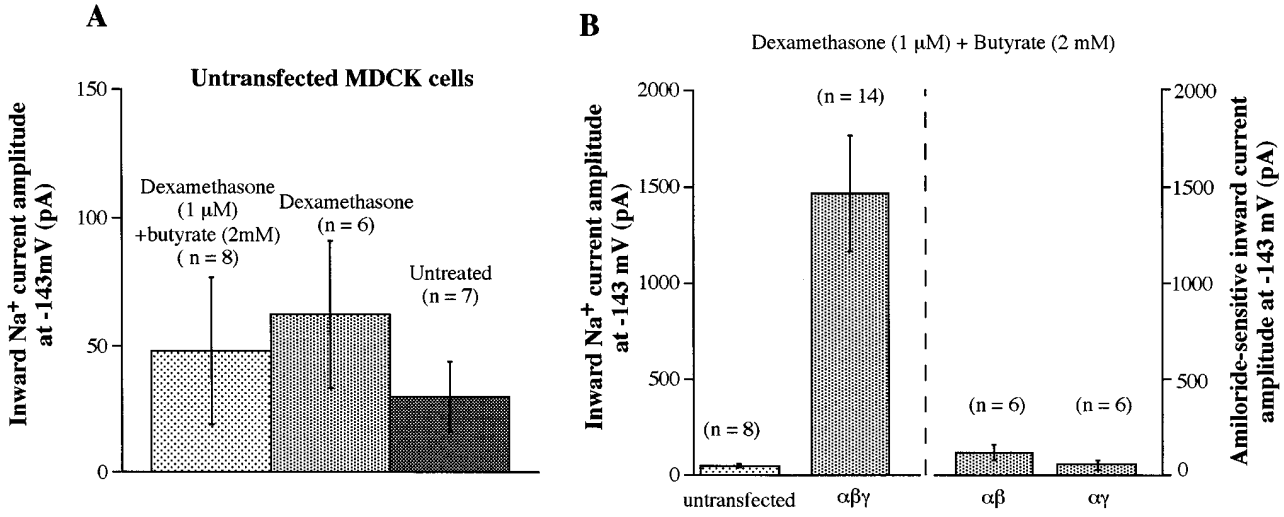

FIGURE 1. (*A*) Inward Na^+ current amplitude at −143 mV measured in untransfected MDCK cells after overnight treatment with 2 mM butyrate and/or 1 μM dexamethasone. The Na^+ current was measured by changing the bath solution from Na-glutamate-rich solution to a solution in which Na^+ had been replaced by equimolar amounts of the impermeant $NMDG^+$ cation. Values are mean ± SEM of six to eight experiments. (*B, left*) Comparison of whole-cell Na^+ conductance in untransfected and αβγrENaC-(stably) transfected MDCK cells after overnight treatment with 2 mM butyrate and 1 μM dexamethasone. All the Na^+ current in the αβγrENaC-transfected MDCK cells is amiloride sensitive, as shown in Fig. 2. Values are mean ± SEM of 8 and 14 experiments, respectively. (*right*) Amiloride (10 μM)-sensitive whole-cell currents in αβ- or αγrENaC stably transfected MDCK cells. Cells were treated overnight with 2 mM butyrate + 1 μM dexamethasone. Inward current amplitude was measured at −143 mV. Values are mean ± SEM of six experiments.

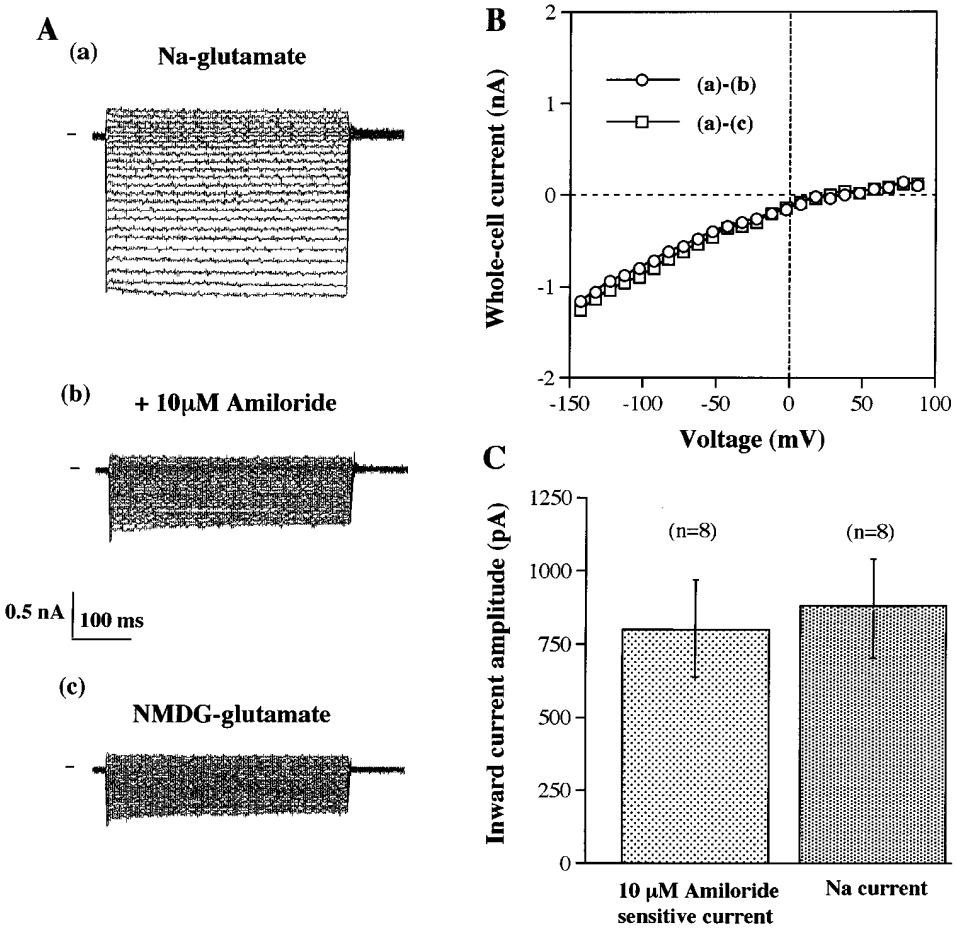

FIGURE 2. (*A*) Representative tracings of whole-cell currents obtained from αβγrENaC-expressing MDCK cells. The cell was held at a potential of +37 mV between test voltage pulses (−143 to +87 mV). The pipette was filled with a standard Cs-glutamate-rich solution. Whole-cell I-V relation was measured when the bath contained a Na-glutamate-rich solution (*a*), and then replacing the bath with a similar solution containing 10 μM amiloride (*b*), or with an NMDG-glutamate-rich solution (*c*). (*B*) Comparison of steady state I-V relation for the amiloride-sensitive whole-cell (○) and Na^+ (□) currents. (*C*) Comparison of inward current amplitudes at −143 mV for the amiloride-sensitive Na^+ and total Na^+ currents.

from those observed after its addition, we obtained the steady state I-V relation for the component of the whole-cell current attributable to amiloride-sensitive Na^+ channels. The steady state I-V relation for the amiloride-sensitive whole-cell current was then compared with that for the whole-cell Na^+ current estimated in the same cell. As seen in Fig. 2, *B* and *C*, there was no difference between the amiloride-sensitive currents and the Na^+ currents at different membrane potentials, indicating that the whole-cell Na^+ current observed in rENaC-expressing MDCK cells was solely mediated by amiloride-sensitive Na^+ channels. These results are consistent with a previous report that demonstrated a much greater amiloride-sensitive short-circuit current in rENaC-transfected than in -untransfected MDCK cells (Stutts et al., 1995).

Since it has been demonstrated that partial ENaC subunit combinations (αβ or αγ) form amiloride-blockable pores in *Xenopus* oocytes (Canessa et al., 1994; McDonald et al., 1995; McNicholas and Canessa, 1997), such "partial channels" might significantly contribute to the amiloride-sensitive conductance observed in our αβγrENaC-expressing MDCK cells. To test this possibility, we performed additional whole-cell voltage-clamp experiments using αβ- or αγrENaC–expressing MDCK cells. Under the present experimental conditions, however, the αβ- and αγrENaC–expressing cells exhibited a very small amiloride-sensitive conductance, with amiloride-sensitive whole-cell current amplitude of only −115.2 ± 41.4 pA ($n = 6$) and −52.1 ± 24.5 pA ($n = 6$) at −143 mV, respectively (Fig. 1 *B, right*).

We next examined the amiloride sensitivity of the whole-cell Na^+ currents. Fig. 3 *A* shows that the inward currents associated with membrane hyperpolarization were inhibited by amiloride in a dose-dependent manner, and that the amiloride-sensitive currents were inwardly rectifying (Fig. 3 *B*). Fig. 3 *C* summarizes the effect of amiloride on the whole-cell inward current at −103 mV. The K_i for the amiloride effect at this membrane potential was ~20 nM. Since the amiloride block of epithelial Na^+ channels is known to be weakly voltage dependent (Palmer, 1985; Warncke and Lindemann, 1985), we further analyzed the voltage dependence of the block. The data with 0.1 μM amiloride were fitted with an equation derived from Eqs. 1 and 2 (Fig. 3 *D*). According to the Woodhull formalism, this slope parameter equals the valence of the blocking particle times the fraction of membrane potential acting on the particle at its blocking site. A mean slope parameter z'

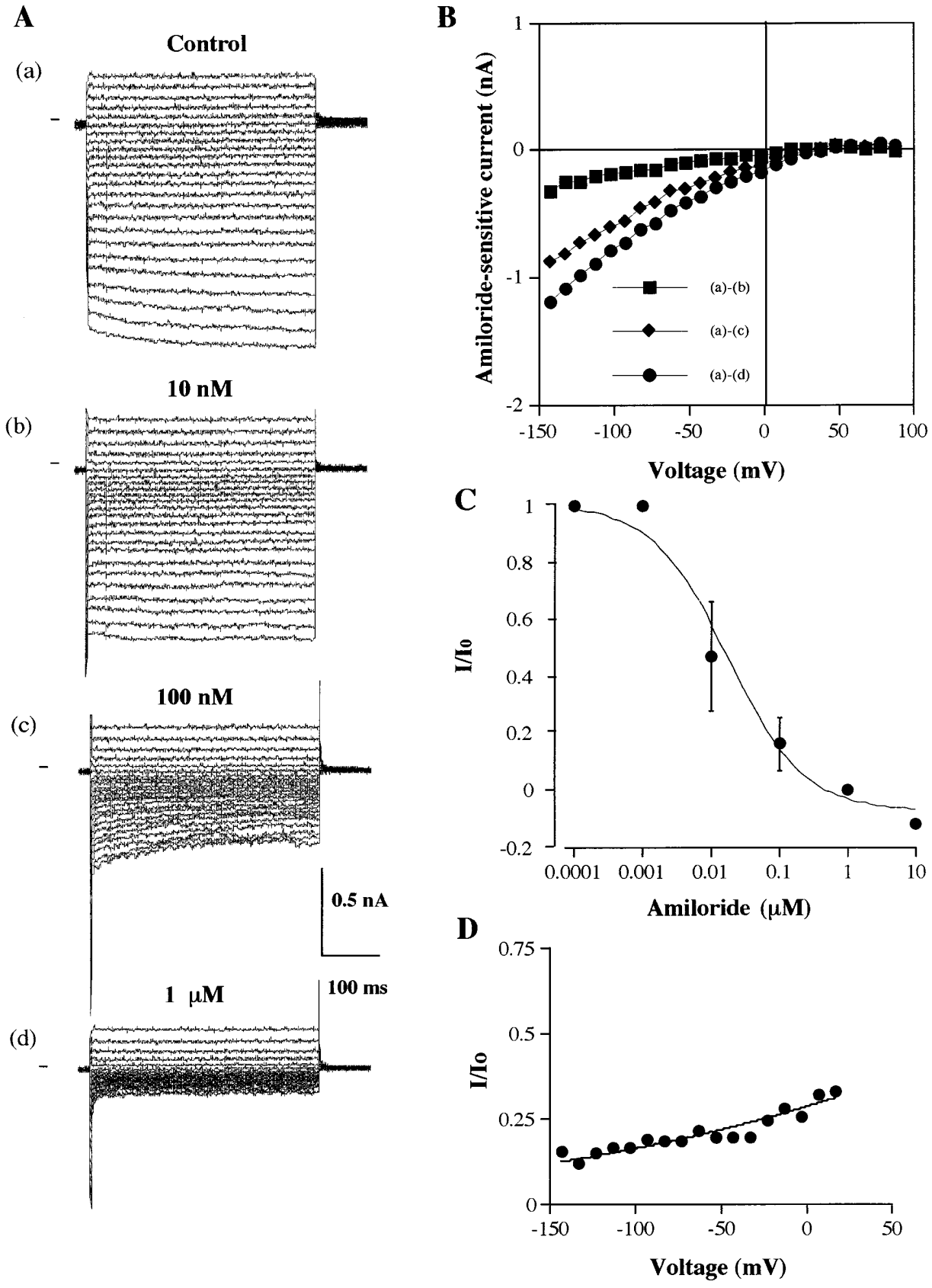
A
Control
(a)
10 nM
(b)
100 nM
(c)
0.5 nA
100 ms
1 μM
(d)
B
Amiloride-sensitive current (nA)
1
0
-1
-2
-150
-100
-50
0
50
100
Voltage (mV)
(a)-(b)
(a)-(c)
(a)-(d)
C
I/Io
1
0.8
0.6
0.4
0.2
0
-0.2
0.0001
0.001
0.01
0.1
1
10
Amiloride (μM)
D
I/Io
0.75
0.5
0.25
0
-150
-100
-50
0
50
Voltage (mV)

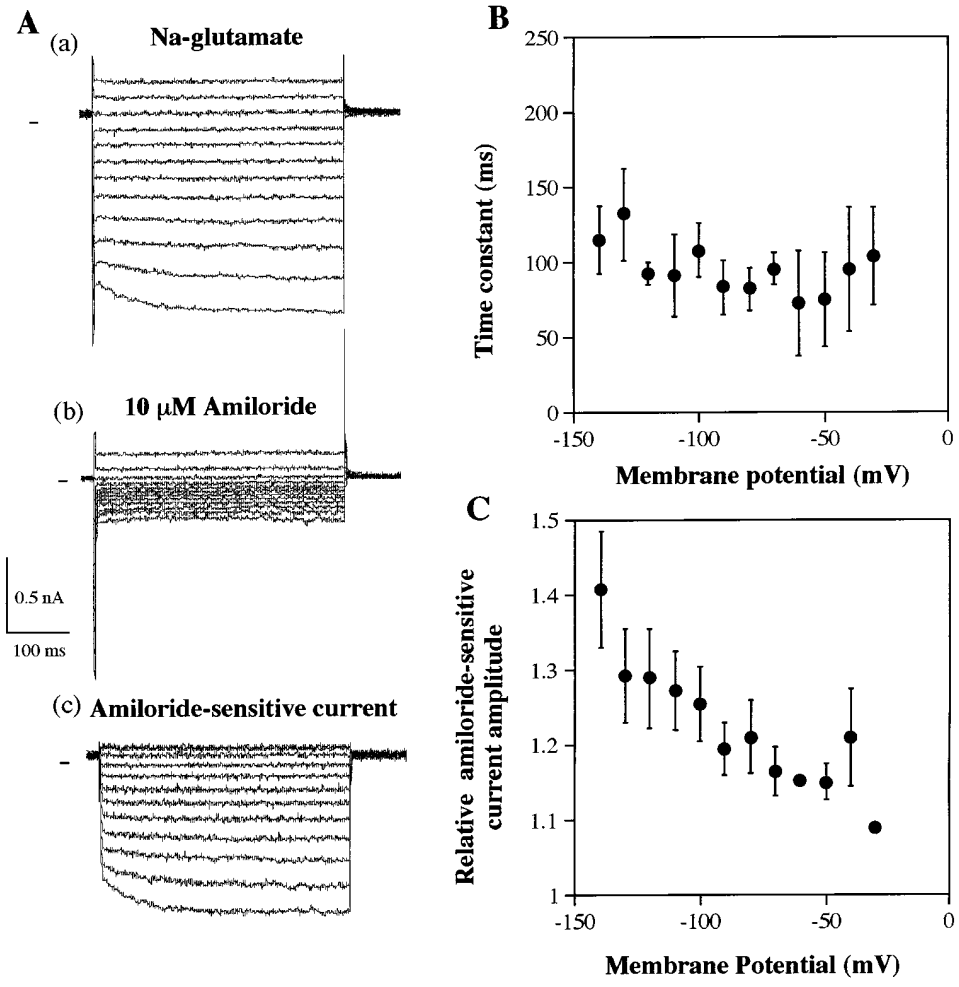

FIGURE 4. Voltage dependence of whole-cell Na^+ conductance in rENaC-expressing MDCK cells. (*A*) An example of tracings of the whole-cell currents (*a*) before and (*b*) after the addition of amiloride (10 μM) to the bath solution. (*c*) Tracings of amiloride-sensitive currents obtained from *a* and *b*. Hyperpolarizing and depolarizing pulses 400 ms in duration were applied from a holding potential of +37 mV to potentials between −143 and +87 mV in 20-mV intervals. The pipette was filled with a Cs-glutamate-rich solution. Dependence of the relaxation time constant (*B*) and amiloride-sensitive current amplitude relative to that at +37 mV (*C*) on the membrane potential estimated from the whole-cell Na^+-current induced by voltage pulses from a resting potential of +37 mV. The relative amiloride-sensitive current amplitude is defined as described in METHODS. Each point represents the mean ± SEM of four to six experiments.

for the voltage dependency of amiloride block was estimated to be 0.20 at 22°C. Therefore, the electrical distance, δ, was 20% of the transmembrane electric field, suggesting that the amiloride-binding site is located within the outer entrance of the ion conductive pathway. This is consistent with recent site-directed mutagenesis experiments of αβγrENaC, suggesting an involvement of a short segment preceding the second membrane spanning domain, which may be within the transmembrane electric field, in channel block by amiloride (Schild et al., 1997).

Voltage Dependence of rENaC Expressed in MDCK Cells

rENaC-expressing MDCK cells exhibited slowly activating currents when the membrane was hyperpolarized to potentials more negative than −100 mV. Fig. 4 *A* shows tracings of the whole-cell currents associated with voltage jumps from a holding potential of +37 mV between −143 and +87 mV before and after addition of amiloride (10 μM) to the bath solution. To characterize the time course of the activation of amiloride-sensitive whole-cell Na^+ currents in these cells, we digitally subtracted the whole-cell currents recorded in the presence of the inhibitor from those recorded in its absence. A relaxation of the whole-cell current when the membrane was strongly hyperpolarized was truly mediated by amiloride-sensitive conductance (Fig. 4 *A*, *c*). To further characterize the relaxation of the whole-cell current, we examined the effect of membrane potential on its relaxation kinetics, which was analyzed as de-

FIGURE 3. Amiloride sensitivity of whole-cell Na^+ currents in rENaC-expressing MDCK cells. (*A*) Representative tracings of the effect of different concentrations of amiloride obtained from a single MDCK cell. The pipette was filled with a standard Cs-glutamate-rich solution, and the bath contained a Na-glutamate-rich solution. The cell was held at a potential of +37 mV between test voltage pulses (−143 to +87 mV). (*B*) The corresponding I-V relations obtained from the same cell shown in *A*. (*C*) Dose-inhibition relation for the amiloride effect at −103 mV. Effect of different concentrations of amiloride (I/I_0) was normalized to a value in the presence of 1 μM amiloride. Data were fitted with Eq. 1 (see METHODS), where $n' = 0.8$. Each point represents the mean ± SEM of two to five experiments. (*D*) Effect of membrane potential on the amiloride inhibition (at 0.1 μM) of the whole-cell current. Data were fitted with an equation derived from Eqs. 1 and 2 (see METHODS). Each point represents the mean of four experiments.

scribed in METHODS. Fig. 4 *B* shows a plot of the relaxation time constant as a function of membrane potential. The time constant did not change significantly at voltages between −143 and −33 mV: the values at −143 and −73 mV were 114.4 ± 23.0 ms (n = 7) and 94.9 ± 11.1 ms (n = 6), respectively. The relative amiloride-sensitive current amplitude was shown to be slightly voltage dependent so that the relative value was 1.41 ± 0.08 (n = 7) at −143 mV and 1.16 ± 0.03 (n = 6) at −73 mV (Fig. 4 *C*).

Since amiloride-sensitive outward current showed a time-dependent activation at markedly depolarized intracellular voltages (+80 mV) when rENaC was expressed in *Xenopus* oocytes (Awayda et al., 1996), we wanted to examine if a similar phenomenon can be observed in rENaC-expressing MDCK cells. To do this, cells were bathed in NMDG-glutamate-rich solution and dialyzed with Na^+-glutamate-rich pipette solution. Under these conditions, however, we found that amiloride-sensitive outward current exhibited a time-dependent inactivation at markedly depolarized voltages (Fig. 5 *A*, *c*). Time constant of the current decay at +68 and +28 mV was 162.8 and 139.4 ms, respectively. The relative amiloride-sensitive current amplitude was 1.25 at +68 mV and 1.13 at +28 mV. These data together support the idea that the channels are activated by membrane hyperpolarization.

Ion Selectivity of the Whole-Cell Na^+ Conductance

With the standard Cs-glutamate-rich pipette solution and Na-glutamate-rich bath solution, the amiloride (10 μM)-sensitive whole-cell currents had a zero-current potential of +63.2 ± 10.5 mV (n = 16). Assuming that the amiloride-sensitive current was carried by Na^+ and Cs^+, the relative permeability of Na^+ to Cs^+ (P_{Na}/P_{Cs}) was estimated to be 11. To characterize the ion selectivity of the macroscopic currents mediated by rENaC ex-

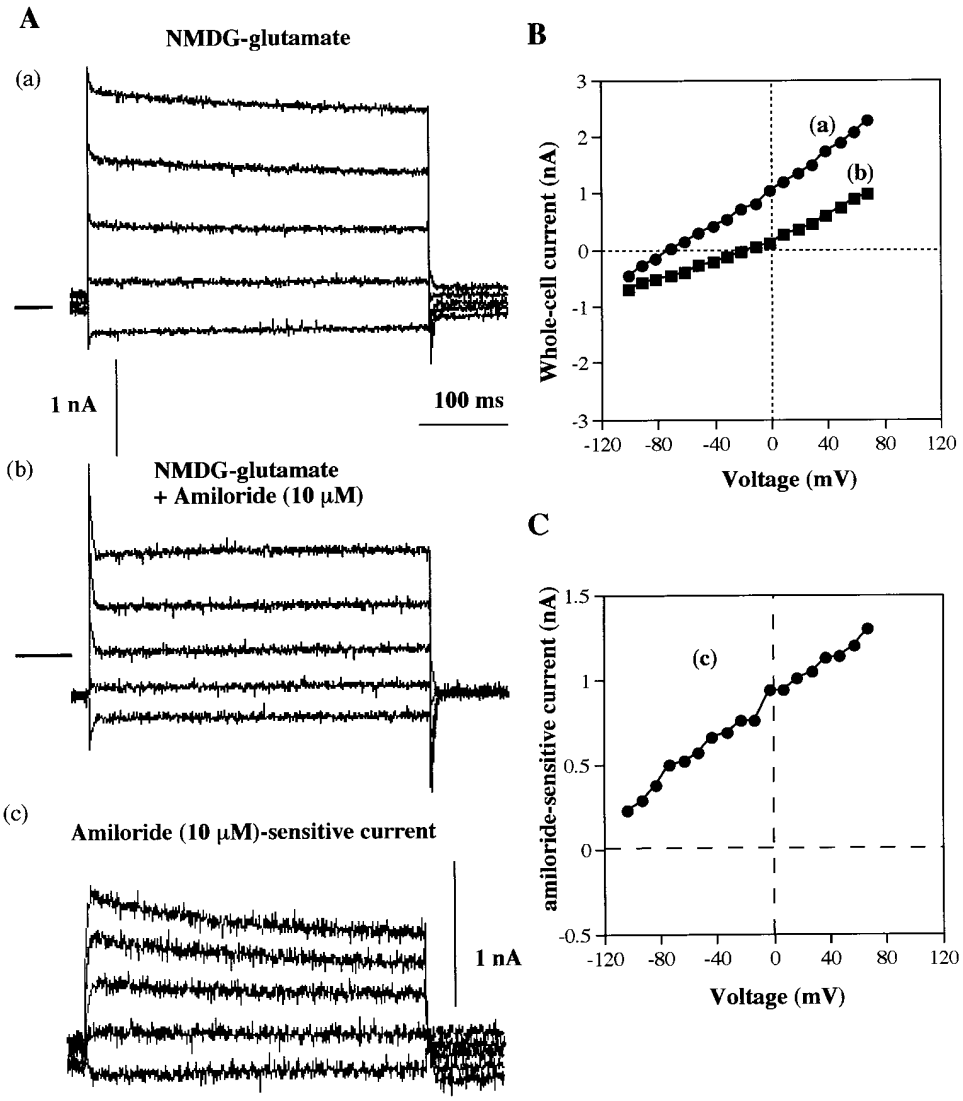

FIGURE 5. (*A*) Whole-cell currents recorded from rENaC-expressing MDCK cells using a Na-glutamate-rich pipette solution. Bath solution was NMDG-glutamate-rich in the absence (*a*) or presence (*b*) of 10 μM amiloride. (*c*) Tracings of amiloride-sensitive currents obtained from *a* and *b*. Hyperpolarizing and depolarizing pulses 400 ms in duration were applied from a holding potential of −62 mV to potentials between −92 and +68 mV in 40-mV intervals. (*B*) The corresponding I-V relations of the whole-cell currents obtained from the same cell shown in *A*. (*C*) The corresponding I-V relation of amiloride-sensitive Na^+ outward currents obtained from the same cell shown in *A, c*.

pressed in MDCK cells, we examined the relative permeabilities for various cations of the whole-cell currents. Fig. 6 *A* shows representative whole-cell current tracings recorded from a single cell. In this experiment, whole-cell currents were recorded in the presence of 150 mM Na^+, $NMDG^+$, K^+, or Li^+ as the glutamate salt in the bathing solution. Replacement of Na^+ with $NMDG^+$ or K^+ failed to support the amiloride-sensitive inward current. When Li^+ was used as the main charge carrier, however, it produced larger inward currents than Na^+, which was completely blocked by amiloride (10 μM). Fig. 6 *B* shows the corresponding I-V relations of the amiloride-sensitive Na^+ and Li^+ currents depicted in Fig. 6 *A*. When the amiloride-sensitive Na^+ and Li^+ currents were measured in the same cells, the corresponding current amplitudes at −143 mV were −0.85 ± 0.15 nA (n = 6) and −1.81 ± 0.33 nA (n = 6), respectively. The ratio of the amiloride-sensitive Li^+ to Na^+ current at this membrane potential was calculated to be 1.94 ± 0.27 (n = 6) (Fig. 6 *C*).

We also ensured that $NMDG^+$ does not pass through the channel in additional experiments in which the cells were bathed in NMDG-glutamate-rich solution and dialyzed with Na^+-glutamate-rich pipette solution. Under these conditions, if $NMDG^+$ could not permeate the channel, amiloride-sensitive current should be outward at all membrane potentials. A zero-current potential of the amiloride-sensitive current could not be observed even at −100 mV, suggesting an extremely low permeability for $NMDG^+$ (Fig. 5 *C*). Given this extremely low permeability, our results with K^+ replacement indicate that the permeability to K^+ is comparable to that of $NMDG^+$ (Fig. 6). From these experiments, we estimated the ion selectivity sequence to be $Li^+ > Na^+ >> K^+ = NMDG^+$.

Single Channel Characteristics of rENaC Expressed in MDCK Cells

To characterize single channel features of rENaC expressed in MDCK cells, which could be responsible for

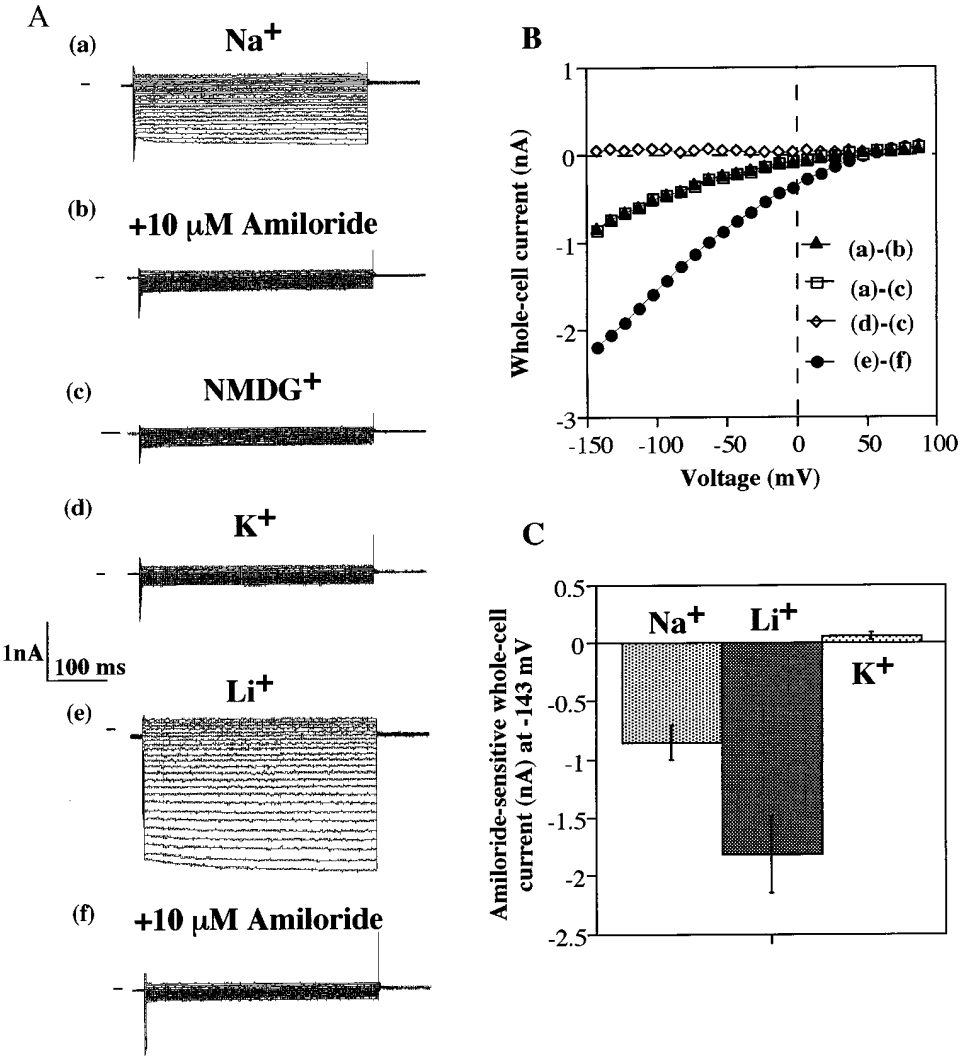

FIGURE 6. Ion selectivity of whole-cell Na^+ conductance in rENaC-expressing MDCK cells. (*A*) Representative tracings of whole-cell currents recorded from rENaC-expressing MDCK cells in the presence of: (*a*) Na^+, (*b*) Na^+ plus 10 μM amiloride, (*c*) $NMDG^+$, (*d*) K^+, (*e*) Li^+, or (*f*) Li^+ plus 10 μM amiloride (150 mM of each cation as the glutamate salt in the bathing solution). The pipette solution was filled with a Cs-glutamate-rich solution. Hyperpolarizing and depolarizing pulses 400 ms in duration were applied from a holding potential of +37 mV to potentials between −143 and +87 mV in 10-mV intervals. (*B*) The corresponding I-V relations of the amiloride-sensitive Na^+ and Li^+ currents shown in *A*. (*C*) Comparison of amiloride (10 μM)-sensitive Na^+ and Li^+ currents at −143 mV. K^+ currents were estimated by subtraction of whole-cell current in the presence of 150 mM K^+ from that in the presence of 150 mM $NMDG^+$. The amiloride-sensitive Na^+ and Li^+ currents were measured in the same cells. Data are the mean ± SEM of six experiments.

the whole-cell currents, we performed single-channel current measurement. We first used an outside-out patch configuration to study the single channel conductance attributable to rENaC, because this configuration allows measurement of the single channel current under the same ionic conditions as those performed with whole-cell recordings. The patch pipette was filled with a Cs-glutamate solution and the bath contained Li-glutamate-rich solution as in the whole-cell experiments. Under these conditions, we usually observed multiple openings of Na^+ channels in patches from the rENaC-expressing cells. Fig. 7 *A* demonstrates the presence of amiloride-sensitive single channel currents in an outside-out patch. In this patch, single channel current transitions with up to four channel levels could be observed. Application of amiloride (10 μM) abolished channel activity. This effect was reversible upon washout of amiloride. To characterize amiloride-sensitive single channel conductance, we next determined the I-V relation of the channel. Such I-V relation from nine experiments are summarized in Fig. 7 *B*. Based on these results, the single channel conductance was estimated to be 8.1 ± 0.7 pS (n = 9) for Li^+ under these experimental conditions. A reversal potential of the current was deviated far from 0 mV, suggesting that Li^+ permeability of the channel was much greater than Cs^+, although the relative permeability of Li^+ to Cs^+ could not be determined experimentally. We also found that the single-channel conductance was reduced by replacement of Li^+ with Na^+ in the bath solution (Fig. 7 *C*), indicating a greater permeability of Li^+ over Na^+. The single channel conductance for Na^+ was 4.7 ± 0.6 pS (n = 4). We could not detect any current transition when K^+ was substituted for Li^+ (data not shown). In cell-attached and inside-out patches, we also found similar single channel currents to those in outside-out patches. In cell-attached patches, single channel conductance of the inward current was 8.6 ± 0.9 pS (n = 3) and 4.7 ± 0.5 pS (n = 7) when Li^+ and Na^+ were used as a charge carrier, respectively.

As expected from the whole-cell voltage-clamp experiments, we found that channel activity was increased upon membrane hyperpolarization. Fig. 8, *A* and *B*, shows representative tracings of a single channel inward current and the corresponding I-V relation in excised inside-out patches. The pipette and bath contained Li-glutamate- and K-glutamate-rich solutions, respectively. In this experiment, the channel activity defined as nP_o at a holding potential of +20, 0, −40, and −80 mV were 0.15, 0.23, 0.40, and 0.78, respectively. Fig. 8 *C* shows the results of six different experiments where nP_o was determined at various membrane potentials. Although the absolute value of nP_o was variable between each experiment, it was consistently increased upon membrane hyperpolarization. When nP_o value was normalized to a value of 1 at −10 mV, the relative nP_o was 2.02 ± 0.86 (n = 6) at −40 mV ($P <$ 0.034) and 3.19 ± 0.52 (n = 4) at −80 mV ($P <$ 0.025), respectively.

As previously shown in whole-cell patch-clamp experiments (Fig. 4 *B*), the voltage-dependent relaxation was apparent when the membrane was hyperpolarized. We

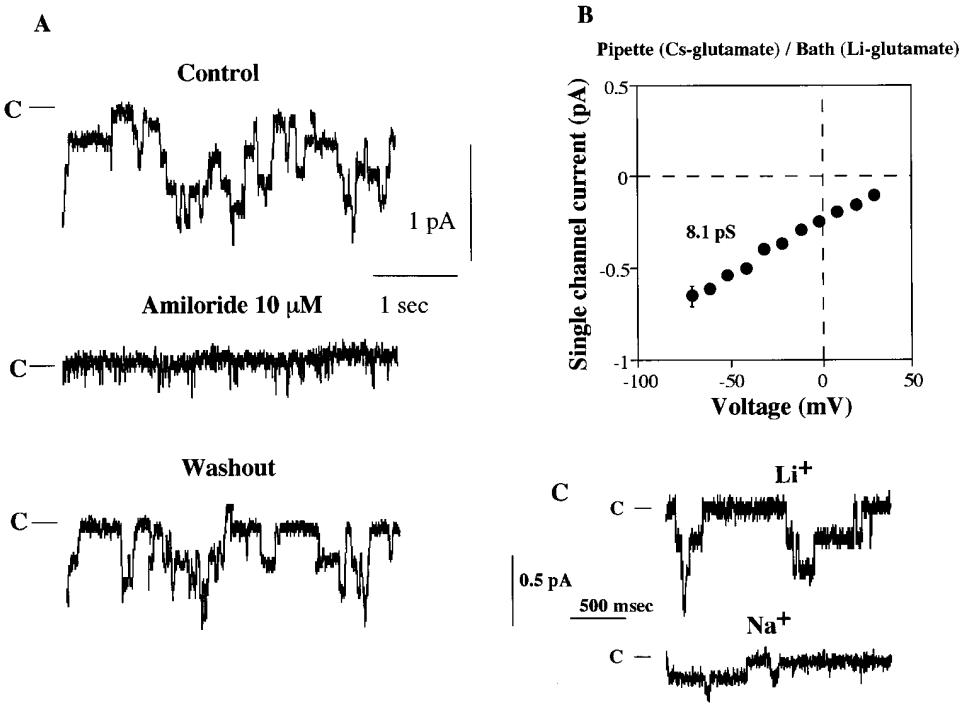

FIGURE 7. (*A*) Amiloride-sensitive single channel recorded in an outside-out patch from rENaC expressed in MDCK cells. The patch pipette was filled with Cs-glutamate solution and the bath contained Li-glutamate-rich solution. Application of amiloride (10 μM) to the bath solution abolished channel activity. Holding potential was −4 mV. (*B*) Current–voltage relation for the amiloride-sensitive single channel current in outside-out patches. The pipette was filled with a Cs-glutamate-rich solution and the bath contained a Li-glutamate-rich solution. Each point represents the mean ± SEM of nine experiments. (*C*) Single channel current traces from an outside-out patch in the presence of 150 mM Li^+ or Na^+ as the glutamate salt in the bathing solution. Holding potential was −4 mV.

also confirmed this property using an inside-out patch. With Li-glutamate-rich solution in the pipette and NMDG-glutamate-rich solution in the bath, we performed an ensemble analysis. Membrane potential was held at +24 mV, and then stepped to −136 mV. When this voltage pulse was repeated 18 times, the corresponding averaged current response showed a slowly activating current (Fig. 9), with a time constant estimated to be 102 ms. This relaxation time constant was similar to that observed in the whole-cell experiments (Fig. 4 *C*). Taken together, these results strongly suggest that this amiloride-sensitive single channel current likely contributes to the amiloride-sensitive whole-cell current observed in the rENaC-expressing MDCK cells.

Extracellular Na^+ Dependency of the Whole-cell Na^+ and Single Channel Conductance

One of the mechanisms proposed for the regulation of luminal Na^+ entry in native Na^+ transporting epithelia is a self-inhibition of channels by extracellular Na^+ (for review see Garty and Palmer, 1997). To test whether extracellular Na^+ concentrations could regulate Na^+ channel activity, we first examined the dependence of the whole-cell Na^+ current on extracellular Na^+ in our rENaC-expressing cells. Fig. 10 *A* shows representative tracings of whole-cell currents from a single cell in the presence of increasing concentrations of extracellular Na^+. The Na^+ concentration was varied by equimolar replacement with $NMDG^+$. In this experiment, whole-cell currents were recorded in the presence of 150 mM Na^+, and then extracellular Na^+ concentration was changed to 0, 5, 10, 30, 75, and 100 mM. Our results show that the inward current declined with decreasing extracellular Na^+ concentration (Fig. 10 *A*). To obtain I-V relationships for the component of the whole-cell current attributable to the Na^+ conductance, the steady state I-V relation of the whole-cell currents was measured in the absence of extracellular Na^+, and then

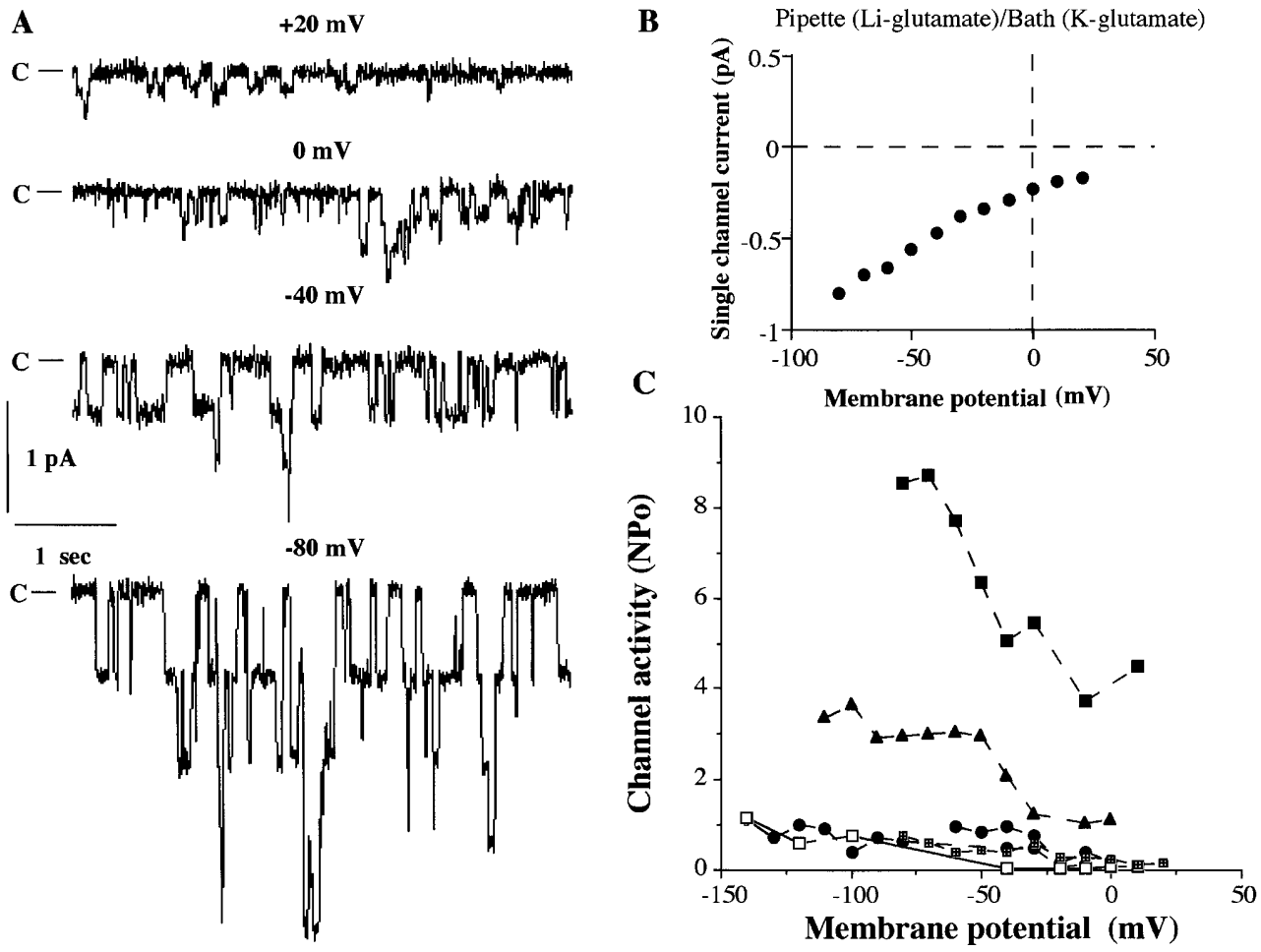

FIGURE 8. Voltage dependence of single channel activity in inside-out patches. (*A*) Representative tracings of a single channel inward current at various membrane potentials, and (*B*) the corresponding I-V relation. (*C*) Summary of six different experiments where nP_o was determined at various membrane potentials. Lines connect data obtained from the same patch. The pipette was filled with a Li-glutamate-rich solution, and the bath contained a K-glutamate-rich solution.

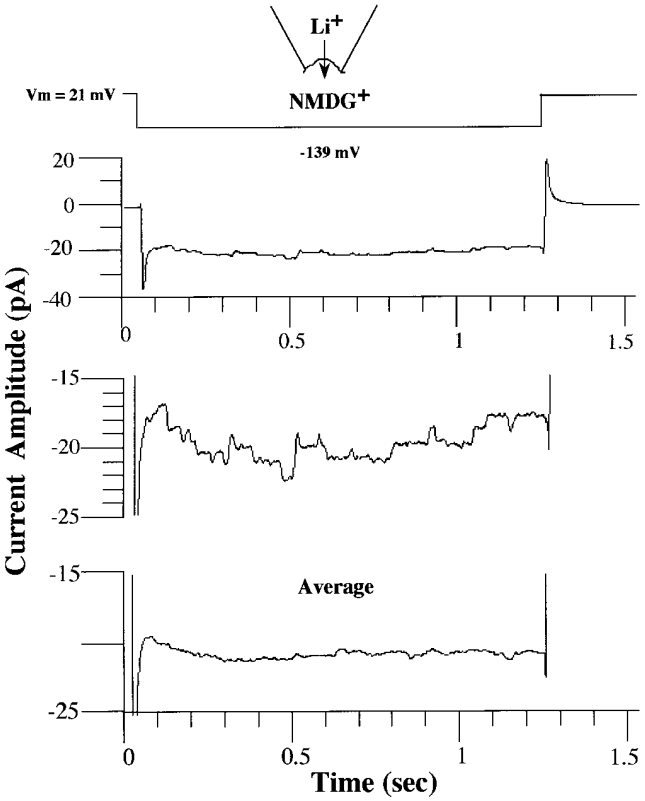

FIGURE 9. An ensemble analysis of single channel current in an excised inside-out patch. The pipette was filled with a Li-glutamate-rich solution and the bath solution was NMDG-glutamate rich. The membrane potential was held at +21 mV and then stepped to −139 mV. Top and middle traces represent the same current response to the voltage-step in different magnification. Lower trace represents the averaged current response when this voltage pulse was repeated 18 times.

subtracted from those observed in the presence of various concentrations of external Na^+. Fig. 10 *B* shows the I-V relations of whole-cell currents in different extracellular Na^+ concentrations obtained for the same cell shown in Fig. 10 *A*. When the current amplitude at −53 mV was normalized to the value at 150 mM Na^+, plotting the normalized inward Na^+ current amplitude as a function of extracellular Na^+ concentration revealed a saturating relation (Fig. 10 *C*). When the data were fitted by the Michaelis-Menten equation, K_m and I_{max} were estimated to be 30.5 mM and 1.14 pS, respectively. At −103 mV, we also observed a similar saturating relation, which could be described by the Michaelis-Menten equation (K_m and I_{max} were 23.1 mM and 1.06 pS, respectively). Furthermore, when normalized whole-cell conductances between −53 and −103 mV to the value at 150 mM Na^+ were plotted as a function of extracellular Na^+ concentration, a similar relation was also observed (K_m = 14.2 mM and G_{max} = 0.99) (Fig. 10 *D*).

To examine the Na^+ dependency of the single channel conductance, we performed single-channel current recording using various concentrations of Na^+ in the pipette solution, and pooled the data from different patches. Since outside-out patches were difficult to maintain for a long enough time to complete the whole protocol, we instead used cell-attached and inside-out patches for this series of experiments. Fig. 11 *A* shows a representative single channel recording in a cell-attached patch configuration. The pipette solution was filled with a low Na solution (29 mM Na^+) and the bath solution contained 150 mM K-glutamate. When the single channel conductance of the inward current was plotted against Na^+ concentrations in the pipette solution, it saturated with increasing Na^+ concentrations, yielding K_m and I_{max} values of 24.4 mM and 5.1 pS, respectively (Fig. 11 *B*). The K_m value observed in these experiments was in agreement with that in the whole-cell experiments above.

Intracellular Na^+ Dependency of the Single Channel Conductance of the Outward Current

We also characterized cytosolic Na^+ dependency of the single channel conductance of the outward current using the inside-out patch configuration. In these experiments, the pipette was filled with a Cs-glutamate-rich solution and the bath solution contained increasing concentrations of Na^+. Single channel conductance of the outward current was 4.2 ± 0.5 pS (n = 8), when Na^+ was used as a charge carrier (Fig. 11 *C*). The channel responsible for the outward current was also permeable to Li^+ ($P_{Li} > P_{Na}$), but not to K^+ (data not shown). When the single channel conductance of the outward current was plotted against cytosolic Na^+ and fitted with the Michaelis-Menten equation, the K_m and I_{max} values were 39.5 mM and 5.1 pS, respectively (Fig. 11 *D*).

Effect of Cytosolic Na^+ Concentration on Channel Activity

We next investigated the effects of cytosolic Na^+ on the gating of single channel currents in excised inside-out patches. The pipette solution was Li-glutamate-rich, and the bath solution contained 0 or 50 mM Na^+ by substituting with $NMDG^+$. 1 mM EGTA was added to the bath solution to ensure low free Ca^{2+} concentrations. Fig. 12, *A* and *B*, shows representative tracings for the effect of Na^+ concentration on channel activity. After excision of the patches, and ensuring that channel activity was stable (see also Fig. 14 *A*), we systematically changed the cytosolic Na^+ levels. As shown in Fig. 12 *A*, increasing cytosolic Na^+ concentration from 0 to 50 mM decreased channel activity and, conversely, decreasing cytosolic Na^+ from 50 to 0 mM increased channel activity (Fig. 12 *B*). Analysis of the current–voltage relationship showed that the single channel conductance of the inward current was not affected by

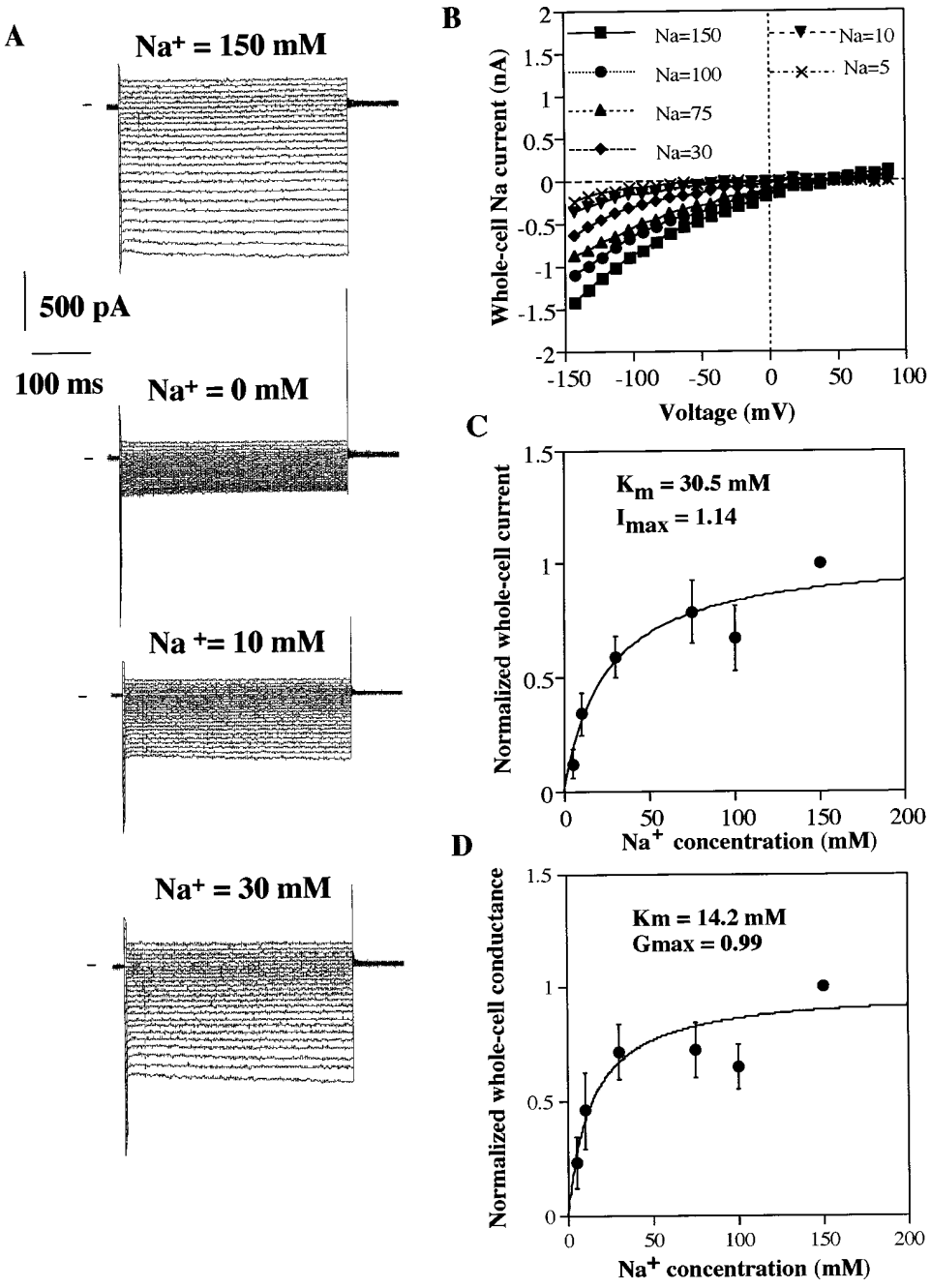

FIGURE 10. Extracellular Na^+ concentration dependency of the whole cell Na^+ current. (*A*) Representative tracings of whole-cell currents from a single cell in the presence of increasing concentrations of extracellular Na^+. The concentration was varied by equimolar replacement with $NMDG^+$. (*B*) The I-V relations of whole-cell currents in different extracellular Na^+ concentrations obtained for the same cell shown in *A*. (*C*) Plot of the inward Na^+ current at −53 mV as a function of extracellular Na^+ concentration. The current was normalized to the value at −143 mV. The data were fitted by the Michaelis-Menten equation (*solid line*). Each point represents the mean ± SEM of three to nine experiments. (*D*) Plot of the normalized whole-cell Na^+ conductance as a function of extracellular Na^+ concentration. The data were fitted by the Michaelis-Menten equation (*solid line*). Each point represents the mean ± SEM of three to nine experiments.

cytosolic Na^+ concentration (data not shown). Fig. 12 *C* summarizes these experiments. Despite variability in the absolute nP_o value between experiments, this value was consistently decreased when the cytosolic Na^+ concentration was increased from 0 to 50 mM. When the nP_o value was normalized to 1 with 0 mM Na^+, the relative nP_o with 50 mM Na^+ was 0.49 ± 0.07 ($n = 8$) ($P < 0.0002$) (Fig. 12 *D*). Conversely, the absolute nP_o value was also consistently increased when the cytosolic Na^+ concentration was decreased from 50 to 0 mM. When the nP_o value was normalized to 1 with 0 mM Na^+, the relative nP_o with 50 mM Na^+ was 0.40 ± 0.09 ($n = 7$, $P < 0.0007$). With cytosolic 100 mM Na^+, the relative nP_o was 0.33 ± 0.19 ($n = 4$, $P < 0.038$) (Fig. 12 *D*). Taken together, these results strongly suggest that cytosolic Na^+ concentrations may regulate the gating properties of rENaC expressed in MDCK cells.

Effect of Cytosolic Ca^{2+} on the Whole-Cell Na^+ Conductance and on Single Channel Activity

Extensive work had previously demonstrated the effect of Ca^{2+} on Na^+ channel activity in native Na^+-transporting epithelia (reviewed by Chase, 1984). We therefore investigated whether rENaC activity is affected by cyto-

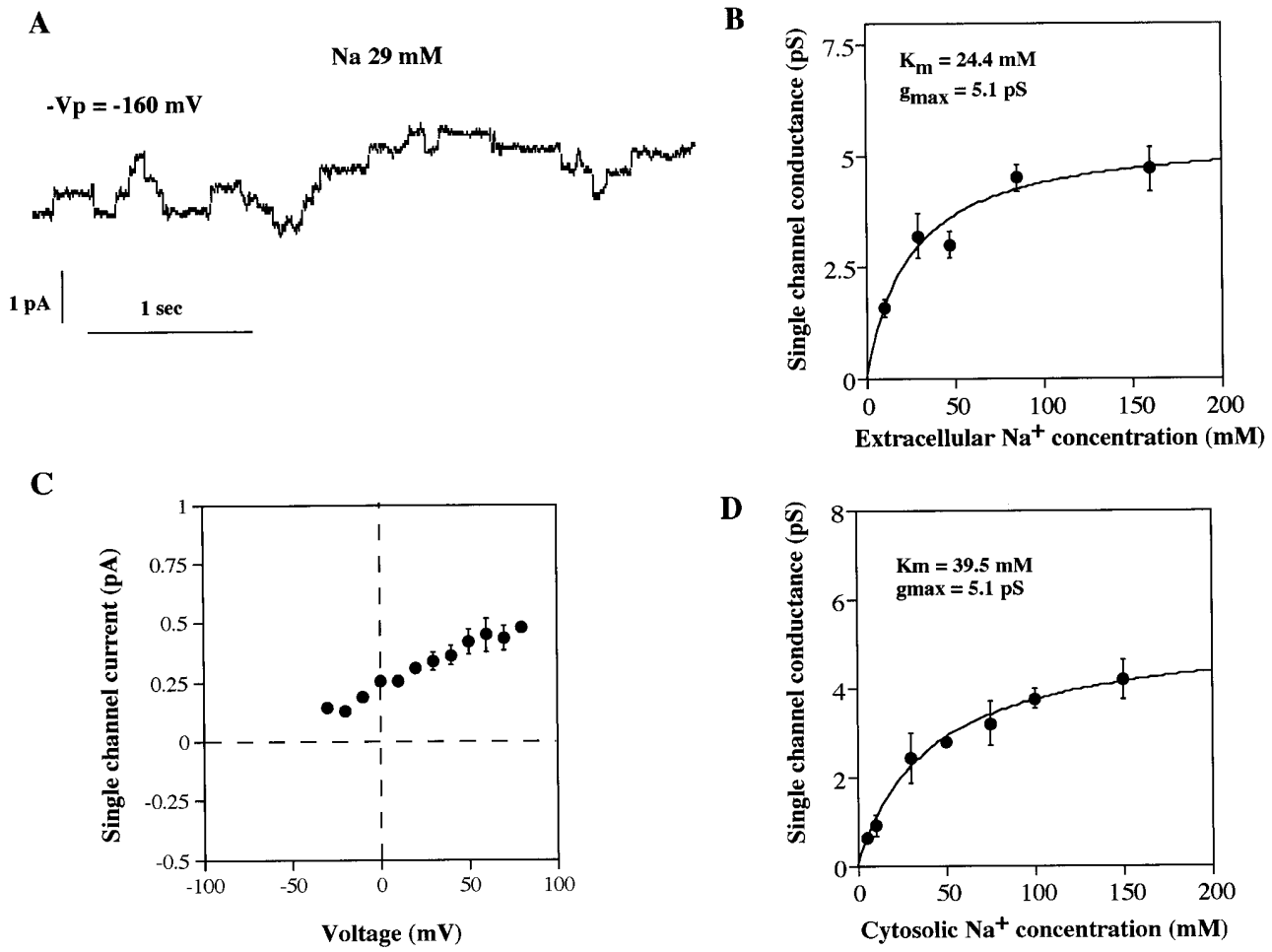

FIGURE 11. Na^+ concentration dependency of the single channel conductance. (*A*) Extracellular Na^+ concentration dependency of the single channel conductance of the inward current. A representative single channel recording in a cell-attached patch. The pipette solution was filled with a low (29 mM) Na^+ solution and the bath solution contained 150 mM K-glutamate. Pipette potential was held at +160 mV. (*B*) Plot of single channel conductance of inward current as a function of Na^+ concentrations in the pipette solution. The data were fitted by the Michaelis-Menten equation (*solid line*). Each point represents the mean ± SEM of three to eight experiments. Intracellular Na^+ concentration dependency of the single channel conductance of the outward current: (*C*) current–voltage relation for single channel outward Na^+ current in inside-out patches. The pipette solution was filled with a Cs-glutamate-rich solution and the bathing solution contained 150 mM Na-glutamate. Each point represents the mean ± SEM of nine experiments. (*D*) Intracellular Na^+ concentration dependency of single channel conductance of outward current in excised inside-out patches. Single channel conductance of outward current is plotted as a function of Na^+ concentrations in the bathing solution. The pipette solution was filled with a Cs-glutamate-rich solution and the bathing solution contained various concentrations of Na^+. The data were fitted by the Michaelis-Menten equation (*solid line*). Each point represents the mean ± SEM of three to nine experiments, except the data of 50 mM Na^+ ($n = 1$).

solic Ca^{2+} levels using whole-cell and single channel current recording techniques. In whole-cell experiments, ramp command voltages were applied from −104 to +76 mV every 30 s. We used this protocol since the reversal potential of the whole-cell current can be estimated, so that any appearance of other conductances, including leak conductance, could be easily identified. First, we performed experiments where ionomycin (1 μM) was used to increase cytosolic Ca^{2+} levels. This concentration of ionomycin has been shown to increase cytosolic Ca^{2+} in MDCK cells under conventional whole-cell patch-clamp configuration (Delles et al., 1995). Fig. 13 *A* shows the instantaneous current–voltage relation of the whole-cell current obtained from a single MDCK cell expressing rENaC. The reversal potential of the whole-cell current was clearly positive, suggesting that the current was carried by Li^+. An example of control experiments is shown in Fig. 13 *B* and summarized in Fig. 13 *C*. The addition of 1 μM ionomycin and 1 mM Ca^{2+} to the bath solution induced an inhibition of the whole-cell inward Li^+ current (Fig. 13 *D*). Time constant of the inhibition was 16.9 ± 1.6 min ($n = 3$). Since we did not perform simultaneous measurements of inward current and cytosolic Ca^{2+} concentration in the same cells, we could not directly evaluate how much cytosolic Ca^{2+} increase was

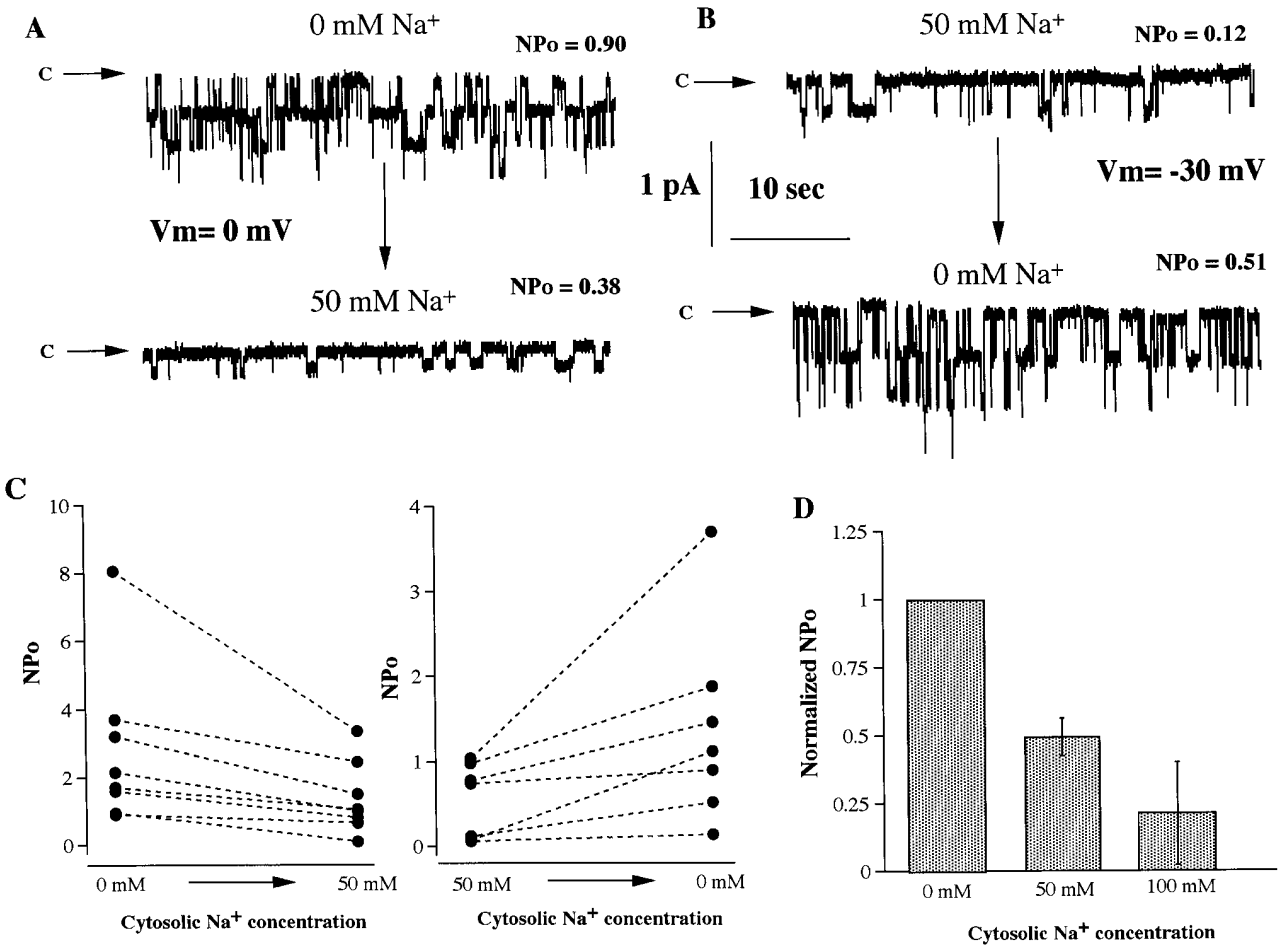

FIGURE 12. Effect of cytosolic Na^+ concentration on single channel activity. (*A* and *B*) Representative tracings in an excised inside-out patch. The pipette was filled with a Li-glutamate-rich solution. (*A*) The effect of increasing cytosolic Na^+ concentration from 0 to 50 mM, and (*B*) the effect of decreasing cytosolic Na^+ concentration from 50 to 0 mM. Holding potentials were 0 and −30 mV, respectively. 1 mM EGTA was added to the bath solution to ensure low Ca^{2+} concentrations. (*C*) Summary of the effect of cytosolic Na^+ concentration (50 mM) on single channel activity. Data were the mean ± SEM of seven or eight experiments. (*D*) Effect of increasing cytosolic Na^+ concentration from 0 to 50 or 100 mM. Data were the mean ± SEM of four or eight experiments.

achieved under the above experimental conditions. We therefore performed additional experiments where free Ca^{2+} concentration in the pipette solution was fixed at 1 μM using 10 mM EGTA to clamp the cytosolic Ca^{2+} concentration. Fig. 13 *E* shows the representative experiment, where the effect of 1 μM Ca^{2+} (pCa = 6) on the whole-cell current was examined. In this experiment, current recording began 3 min after whole-cell dialysis. Our results show that perfusion of the cytoplasm with a pipette solution containing 1 μM Ca^{2+} induced a biphasic inhibition of the current. When the time course of the inhibition was fitted with a double exponential curve, the mean time constants of the fast and slow components were 1.7 ± 0.3 min (n = 3) and 128.4 ± 33.4 min (n = 3), respectively.

To examine the effect of cytosolic Ca^{2+} concentrations on the single channel conductance and gating, we performed additional inside-out patch experiments. Although channel activity usually runs down after excision of the patch membrane, it does tend to reach a steady level 10–45 min after excision (Fig. 14 *A*). Only channels that achieved steady levels were included in the experiment. Fig. 14 *B* shows that an increase in cytosolic Ca^{2+} concentration led to a decrease of channel activity. In this experiment, nP_o was decreased from 0.5 to 0.15 when cytosolic Ca^{2+} was increased from <1 nM to 1 μM. When the nP_o value was normalized to 1 with pCa > 9, increasing cytosolic Ca^{2+} to 1 or 10 μM led to a significant decrease in nP_o (0.65 ± 0.08, n = 8, $P <$ 0.005), and (0.45 ± 0.13, n = 8, $P < 0.005$), respectively (Fig. 14 *C*). However, when cytosolic Ca^{2+} was increased from <1 nM to 0.1 μM, no significant change in nP_o was observed (normalized nP_o value was 1.07 ± 0.11, n = 4, P = 0.58) (Fig. 14 *C*). Analysis of current–voltage relation showed that increasing cytosolic Ca^{2+} from <1 nM to 1 or 10 μM did not affect the single

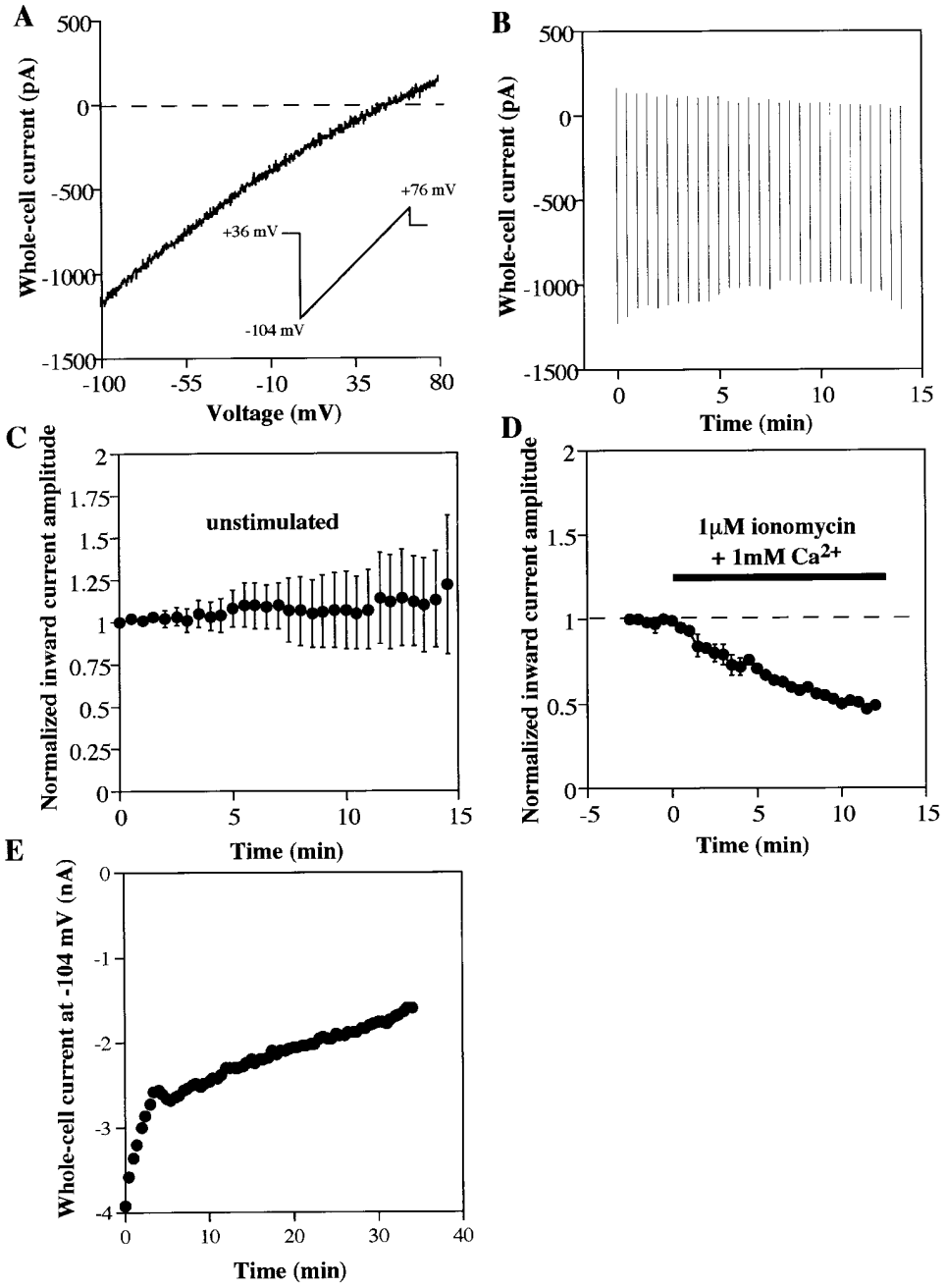

FIGURE 13. Effect of ionomycin on whole-cell current. (*A*) Instantaneous I-V relation of the whole-cell current obtained from a single MDCK cell expressing rENaC. Ramp command voltages were applied from −104 to +76 mV every 30 s. The pipette was filled with a Cs-glutamate-rich solution with 1 mM EGTA, and the bath solution contained Li-glutamate (nominally Ca^{2+} free). (*B*) An example of experiments in unstimulated cells. Ramp command voltages were applied from −104 to +76 mV every 30 s. (*C*) Summary of control experiments. $t = 0$ min corresponds to 3.9 ± 0.4 min ($n = 9$) after whole-cell dialysis. Each point represents the mean ± SEM of three to nine experiments. (*D*) Effect of the addition of ionomycin (1 μM) and 1 mM Ca^{2+} to the bath solution (nominally Ca^{2+} free). Experimental condition was the same as in *A*. Each point represents the mean ± SEM of three experiments. (*E*) The effect of cytoplasm perfusion with 1 μM Ca^{2+}. Representative experiment, where the effect of 1 μM Ca^{2+} in the pipette solution on whole-cell current was examined. In this experiment, the current recording began 3 min after whole-cell dialysis. Ramp command voltages were applied from −104 to +76 mV every 30 s. When time course of the inhibition was fitted with a double exponential, the corresponding time constants of the two components were 1.3 and 64.3 min, respectively. The pipette was filled with a Cs-glutamate-rich solution (pCa = 6), and the bath solution contained Li-glutamate (nominally Ca^{2+} free).

channel conductance (data not shown). Collectively, these results suggest that cytosolic Ca^{2+} inhibits rENaC activity.

DISCUSSION

Although a previous study showed that rENaC stably transfected in MDCK cells exhibits a much greater amiloride-sensitive short circuit current than that in untransfected cells (Stutts et al., 1995), detailed electrophysiological properties of rENaC expressed in these cells have not been determined. Using patch-clamp techniques, we have now characterized rENaC heterologously expressed in these cells and demonstrated regulation of rENaC activity by cytosolic Na^+ and Ca^{2+} concentrations. To our knowledge, this is the first electrophysiological characterization of the cloned ENaC expressed in mammalian epithelial cells.

Comparison of the Biophysical Properties of rENaC Expressed in MDCK Cells to Other Expression Systems

We have demonstrated the presence of functional Na^+ conductance at the plasma membrane of rENaC-expressing cells. This is based on measurement of different levels of whole-cell Na^+ conductance in rENaC-transfected compared with untransfected MDCK cells, the

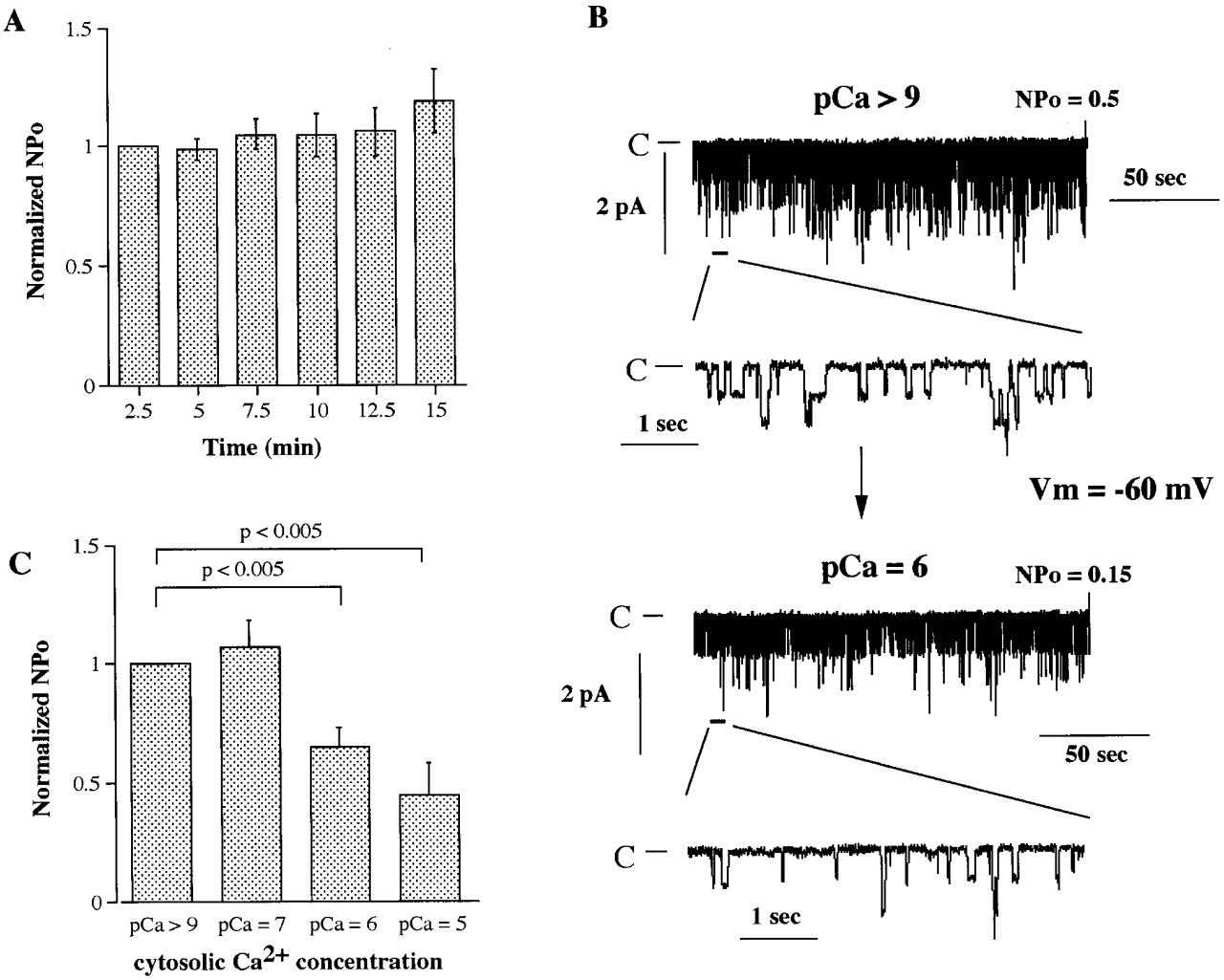

FIGURE 14. (*A*) Stability of Na^+ channel activity in excised inside-out patches. Channel activity was estimated every 2.5 min for 15 min. Pipette solution was filled with Li-glutamate-rich solution and the bath solution contained NMDG-glutamate-rich solution with 1 mM EGTA. Data represent the mean ± SEM of nine experiments. (*B*) Representative experiment, where the effect of increasing cytosolic Ca^{2+} concentration on Na^+ channel activity was examined in an excised inside-out patch. The pipette was filled with Li-glutamate-rich solution and the bath solution contained 150 mM K-glutamate. Holding potential was −64 mV. Cytosolic Ca^{2+} concentration was changed from <1 nM to 1 μM. (*B*) Representative compressed and expanded scale trace for both conditions. (*C*) Effect of cytosolic Ca^{2+} concentrations on channel activity. The nP_o value was normalized to 1 with pCa > 9. Data for pCa = 7, 6, or 5 represent the mean ± SEM of four, eight, or eight experiments, respectively.

sensitivity of the whole-cell Na^+ conductance to amiloride, and the cation selectivity of the whole-cell Na^+ conductance ($Li^+ > Na^+ >> K^+$). Furthermore, our results provide strong evidence that the single channel conductance we identified mediates the whole-cell Na^+ conductance. This is based on the demonstration of shared properties between the single channel and the whole-cell conductances, evident by (*a*) a similar cation selectivity of $Li^+ > Na^+ >> K^+$, (*b*) an inhibition of current by extracellularly applied amiloride, and (*c*) a slight voltage dependence of channel activity. These electrophysiological properties are similar to those reported in *Xenopus* oocytes (Canessa et al., 1994*a*).

In addition to the similarity of biophysical properties between rENaC expressed in MDCK cells and in *Xenopus* oocytes, these two heterologous expression systems seem to be comparable in terms of functional channel density: in *Xenopus* oocytes, assuming a capacitance of 100 nF (Stühmer, 1992) and Na^+ current of 1 μA at −100 mV (Canessa et al., 1994*a*), one can estimate the current density to be 10 pA/pF. Similarly, Na^+ current density in the MDCK cells is 30 pA/pF at −100 mV, since the single cell capacitance of the cells was 33 pF. Furthermore, the present whole-cell voltage-clamp and single channel recording experiments allow estimation of active channel number per cell with an assumption of open probability of the channel in this heterologous

expression system. Taken the values of whole-cell Na^+ current amplitude of 1,000 pA and a single channel current amplitude in outside-out patches of 0.4 pA at −100 mV into account, with an assumption of open probability of 0.5, one can calculate the active channel number to be 5,000 per cell. Since open probability varies between 0 and 1, the minimum number of active channels is estimated to be 2,500 per cell.

The single channel conductance for Na^+ we observed in rENaC expressed in MDCK cells (4.5 pS), which is similar to that observed in *Xenopus* oocytes (4.6 pS) (Canessa et al., 1994*a*), is not consistent with that found in planar lipid bilayers (13 pS) (Ismailov et al., 1996; Awayda et al., 1996). Similarly, unlike previous experiments using lipid bilayers (Ismailov et al., 1996), we could not observe a triple-barrel structure of the single channel conductance in our cells. Currently, there is no simple way to account for this discrepancy. A possible explanation may be the different membrane environment in which the channel is embedded. Accordingly, it is interesting to note that in a recent study performed with lipid bilayers the addition of actin to the solution bathing the *cis* side of αβγrENaC-containing bilayers decreased the conductance from 13 to 7 pS (Ismailov et al., 1997), although the proposed triple-barrel structure of the single channel conductance (Ismailov et al., 1996) cannot be explained by our data.

The present study shows that amiloride-sensitive whole-cell Na^+ current is slowly activated at hyperpolarized membrane potential (Fig. 3). Similar relaxation has been reported in rENaC transiently expressed in *Xenopus* oocytes (Awayda et al., 1996). Our preliminary experiments using αβγrENaC stably expressed in NIH-3T3 cells also showed a similar relaxation of the amiloride-sensitive inward current (our unpublished observations). These observations in three different expression systems suggest that the voltage- and time-dependent activation is an intrinsic property of rENaC. It is interesting to note that in freshly isolated intact rat cortical collecting tubules, such a time-dependent and amiloride-sensitive slowly activating current has been demonstrated in whole-cell recording experiments, although a slower activated current (5–10 s) was also observed in addition to a time constant of relaxation (several hundred milliseconds) (Palmer and Frindt, 1996). The rENaC expressed in MDCK cells, however, seems to be different at least in one significant respect from that reported in *Xenopus* oocytes, where amiloride-sensitive outward current also showed a time-dependent activation at markedly depolarized intracellular voltages (+80 mV) (Awayda et al., 1996). Instead, we observed a time-dependent inactivation of the amiloride-sensitive outward Na^+ current at +68 mV under the present experimental condition (Fig. 5). At this stage, we do not know the reason for this discrepancy.

The underlying assumption in the present study is that the amiloride-sensitive Na^+ whole-cell current observed in αβγrENaC-expressing MDCK cells is mediated by a channel pore made of an αβγ oligomer. This assumption seems valid because αβ- and αγrENaC-expressing MDCK cells exhibited a very small amiloride-sensitive whole-cell conductance relative to that observed in αβγrENaC-expressing cells. Due to these small conductances, not significantly different from those seen in untransfected MDCK cells, we cannot determine whether αβ or αγ oligomers can form a functional channel pore in our cells. It is interesting to note that our own work has shown ubiquitination and proteasomal degradation of rENaC subunits expressed alone or in pairs in mammalian cells (Staub et al., 1997), consistent with the view that partial combination of ENaC subunits may not be targeted efficiently to the plasma membrane (Firsov et al., 1996). Furthermore, a recent study on the stoichiometry of rENaC expressed in *Xenopus* oocytes has demonstrated that the channel pore consists of two α, one β, and one γ chains, and suggested that differential assembly of rENaC subunits into various configurations is unlikely to occur (Firsov et al., 1998).

Regulation of rENaC Activity by Extra- and Intracellular Na^+

The activity of Na^+ channels in the apical membrane of native Na^+-reabsorbing epithelia is known to be controlled by changes in Na^+ concentrations of the extracellular fluid (Garty and Palmer, 1997), although the mechanism by which this intrinsic regulation takes place remains disputed. In the present study, we have shown that the whole-cell Na^+ conductance saturated with increasing extracellular Na^+ concentration. Since the intracellular electrolyte composition can be fixed by the pipette solution, it is unlikely that saturation of whole-cell currents observed here is due to changes in several cytosolic factors including pH, Na^+, and Ca^{2+} concentrations. Although a similar saturation of whole-cell Na^+ currents mediated by rENaC has also been reported in *Xenopus* oocytes (Canessa et al., 1994*a*), the K_m values (23.1 mM at −103 mV) estimated in MDCK cells was different from the 4.9 mM (at −100 mV) found in *Xenopus* oocytes. This may be due to the different experimental conditions, since the above cytosolic factors cannot be well fixed during experiments using the two-microelectrodes voltage-clamp technique, which was applied to *Xenopus* oocytes. On the other hand, it is noteworthy that the K_m of 24.4 mM of rENaC expressed in MDCK cells is in excellent agreement with the K_m of 25 mM reported for the single Na^+ channels in the rat cortical collecting duct (Palmer and Frindt, 1988).

We also showed that the single-channel conductance saturated with increasing extracellular Na^+, and that the dependency (as indicated by K_m) of both whole-cell

and single channel conductances on extracellular Na^+ was comparable. As the macroscopic Na^+ conductance is defined as a product of single channel conductance (g), the number of active channels (n), and open probability (P_o), these results strongly suggest that a saturation of whole-cell Na^+ currents is due to a saturation of single channel conductance of rENaC expressed in MDCK cells. In other words, Na^+ channel activity defined as nP_o should be constant with increasing extracellular Na^+. Therefore, we conclude that saturation of whole-cell current with increased extracellular Na^+ concentrations observed in the present study can be explained by saturation of the single channel conductance. A similar conclusion was reached by a recent study using noise analysis to study amiloride-sensitive whole-cell currents in mouse submandibular duct cells (Komwatana et al., 1996*a*), although the exact molecular identity of the channels in those cells remains unknown. We cannot completely exclude the possibility, however, that extracellular Na^+ concentration may affect Na^+ channel activity since the present whole-cell data do not allow us to determine K_m very precisely. Direct experiments using outside-out patches will be required to make this issue clearer.

The present study provides a direct evidence that cytosolic Na^+ concentration may regulate the gating properties of rENaC, independent of changes in cytosolic pH and Ca^{2+}, although the mechanism by which cytosolic Na^+ can regulate channel activity remains unknown. This is contrary to a previous report showing that Na^+ channel activity in excised patches from rat cortical collecting duct failed to show a significant effect of complete replacement of intracellular-side K^+ with Na^+ (Palmer et al., 1989). Since the biophysical properties of Na^+ channels in this tissue are in excellent agreement with those of rENaC heterologously expressed in MDCK cells and in *Xenopus* oocytes, we do not know the reason for this discrepancy. However, there are two previous studies that revealed an inhibitory effect of cytosolic Na^+ concentration on molecularly undefined, amiloride-sensitive Na^+ channel activities. A direct effect of cytosolic Na^+ concentration on channel activity has been observed in immunopurified bovine medullary Na^+ channels incorporated into planar lipid bilayers (Ismailov et al., 1995), in which the inhibition was observed only when the free Ca^{2+} bathing the cytosolic surface of the channel was above 5 μM. This Ca^{2+} dependency of the Na^+ effect, however, appeared to be distinct from that observed in rENaC expressed in MDCK cells, because the cytosolic bathing solution used in our study contained 1 mM EGTA without added Ca^{2+}. A recent study on amiloride-sensitive whole-cell currents in mouse submandibular duct cells also showed that increasing intracellular Na^+ concentration from 0 to 68 mM caused a significant decrease in channel activity (defined as nP_o) estimated by noise analysis (Komwatana et al., 1996*b*). Thus, our work is in support of the existence of an intracellular Na^+-regulatory (sensing) site(s) in rENaC, although we do not know yet whether this putative site is interacting with Na^+ directly.

Regulation of rENaC Activity by Intracellular Ca^{2+}

A key finding in the present study is the inhibition of rENaC by elevated cytosolic Ca^{2+} concentration. We demonstrated that the whole-cell current mediated by rENaC was decreased by the addition of the Ca^{2+}-ionophore ionomycin (1 μM) to the bath solution, or by perfusion of the cytoplasm with a pipette solution containing 1 μM free Ca^{2+}. We also showed that the single channel activity in excised inside-out patches was inhibited by increasing cytosolic Ca^{2+} concentration from $<$1 nM to 1 μM without changing the single channel conductance. Although the latter results suggest a direct inhibition by Ca^{2+}, we cannot preclude the possibility that the Ca^{2+}-induced inhibition observed in the present whole-cell experiments may also be mediated by an indirect mechanism. One possible indirect mechanism may be the activation of a Ca^{2+}-dependent enzyme such as protein kinase C since PKC was recently shown to downregulate rENaC activity in planar bilayers and in *Xenopus* oocytes (Awayda et al., 1996), as also shown in Na^+ channels from A6 amphibian epithelial cells (Ling and Eaton, 1989). Further detailed studies will be necessary to examine whether inhibition of rENaC activity by cytosolic Ca^{2+} observed in the present study could be mediated by this pathway.

The observation that whole-cell dialysis with the pipette solution containing 1 μM free Ca^{2+} induced a biphasic inhibition of whole-cell currents, an initial rapid (within 5 min) inhibition followed by a secondary slow inhibition (after 5 min), leads us to postulate at least two different modes of the inhibitory action of Ca^{2+} on channel function. One may act on the gating properties of the channel since increasing cytosolic Ca^{2+} to 1 μM was found to decrease channel activity without changing single channel conductance in the excised inside-out patches. Indeed, it was shown previously that increasing free Ca^{2+} concentration of the cytosolic side from $<$1 nM to several tens of micromolar causes an inhibition of open probability of immunopurified bovine renal Na^+ channels reconstituted into lipid bilayer (Ismailov et al., 1995). A direct inhibition of Na^+ channels by micromolar concentrations of Ca^{2+} in the cytoplasmic compartment was also observed in membrane vesicles prepared from toad urinary bladder (Garty et al., 1987). Such a direct effect, however, was not observed in excised inside-out patches from rat cortical collecting duct cells (Palmer and Frindt, 1987), although the addition of a Ca^{2+} ionophore decreased channel activity in cell attached patch-clamp recordings.

The other slower mode of Ca^{2+}-induced inhibition may affect the number of active channels at the plasma membrane. In this regard, it is interesting that we have recently demonstrated that the ubiquitin protein ligase, Nedd4, endogenously expressed in MDCK cells, is translocated to the plasma membrane in response to treatment with ionomycin (1 μM) plus Ca^{2+}, an effect mediated by its C2 domain (Plant et al., 1997). Since we had previously shown that Nedd4 binds rENaC in living cells (Staub et al., 1996) and, independently, that rENaC stability and function is regulated by ubiquitination (Staub et al., 1997), it is possible that this Ca^{2+}-dependent accumulation of Nedd4 at the plasma membrane may be at least partly responsible for the slow inhibitory effect of Ca^{2+} on rENaC activity by decreasing the number of channels at the cell surface. Furthermore, the existence of two such different mechanisms for Ca^{2+}-induced inhibition of the Na^+ channels is not without precedent; previous studies using membrane vesicle preparations indeed suggested the presence of both an indirect and a direct inhibitory effect of Ca^{2+} on Na^+ channels (Garty and Asher, 1985, 1986; Garty et al., 1987).

In conclusion, we have characterized the electrophysiological properties of rENaC heterologously expressed in a mammalian epithelial cell line, and have also provided evidence for the regulation of rENaC by cytosolic Na^+ and Ca^{2+}. This stable expression system may serve as a useful tool to study simultaneously biochemical and functional aspects of the cloned ENaC channel, or mutant channel, when expressed in mammalian epithelial cells.

The authors thank Drs. B. Rossier and C. Canessa for providing the αβγ- and αβrENaC-expressing MDCK cells.

This work was supported by the Canadian Cystic Fibrosis Foundation (to D. Rotin), by the Medical Research Council (MRC) of Canada (to D. Rotin), an MRC Group Grant in Lung Development (to D. Rotin and Y. Marunaka), by a grant from the international Human Frontier Science Program (to D. Rotin), and by the Kidney Foundation of Canada (to Y. Marunaka). T. Ishikawa is supported by a stipend from RESTRACOM. D. Rotin and Y. Marunaka were recipients of a Scholarship from the MRC of Canada.

Original version received 19 November 1997 and accepted version received 16 March 1998.

REFERENCES

Awayda, M.S., I.I. Ismailov, B.K. Berdiev, C.M. Fuller, and D.J. Benos. 1996. Protein kinase regulation of a cloned epithelial Na^+ channel. *J. Gen. Physiol.* 108:49–65.

Barry, P.H., and J.W. Lynch. 1991. Liquid junction potentials and small cell effects in patch-clamp analysis. *J. Membr. Biol.* 121:101–117.

Canessa, C.M., J.-D. Horisberger, and B.C. Rossier. 1993. Epithelial sodium channel related to proteins involved in neurodegeneration. *Nature.* 361:467–470.

Canessa, C.M., L. Schild, G. Buell, B. Thorens, I. Gautschi, J.-D. Horisberger, and B.C. Rossier. 1994*a*. Amiloride-sensitive epithelial Na^+ channel is made of three homologous subunits. *Nature.* 367:463–467.

Canessa, C.M., A.-M. Mérillat, and B.C. Rossier. 1994*b*. Membrane topology of the epithelial sodium channel in intact cells. *Am. J. Physiol.* 267:C1682–C1690.

Chang, S.S., S. Gruender, A. Hanukoglu, A. Roesler, P.M. Mathew, I. Hanukoglu, L. Schild, Y. Lu, R.A. Shimkets, C. Nelson-Williams, B.C. Rossier, and R.P. Lifton. 1996. Mutations in the subunits of the epithelial sodium channel cause salt wasting with hyperkalaemic acidosis, pseudohypoaldosteronism type 1. *Nat. Genet.* 12:248–253.

Chase, H.S., Jr. 1984. Does calcium couple the apical and basolateral membrane permeabilities in epithelia? *Am. J. Physiol.* 247: F869–F876.

Delles, C., T. Haller, and P. Dietl. 1995. A highly calcium-selective cation current activated by intracellular calcium release in MDCK cells. *J. Physiol. (Camb.).* 486:557–569.

Firsov, D., L. Schild, I. Gautschi, A.-M. Mérillat, E. Schneeberger, and B.C. Rossier. 1996. Cell surface expression of the epithelial Na^+ channel and a mutant causing Liddle syndrome: a quantitative approach. *Proc. Natl. Acad. Sci. USA.* 93:15370–15375.

Firsov, D., I. Gautschi, A.-M. Mérillat, B.C. Rossier, and L. Schild. 1998. The heterotetrameric architecture of the epithelial sodium channel (ENaC). *EMBO (Eur. Mol. Biol. Organ.) J.* 17:344–352.

Fuchs, W., E. Hviid-Larsen, and B. Lindemann. 1977. Current–voltage curve of sodium channels and concentration dependence of sodium permeability in frog skin. *J. Physiol. (Camb.).* 267:137–166.

Fuller, C.M., M.S. Awayda, M.P. Arrate, A.L. Bradford, R.G. Morris, C.M. Canessa, B.C. Rossier, and D.J. Benos. 1995. Cloning of a bovine renal epithelial Na^+ channel subunit. *Am. J. Physiol.* 269: C641–C654.

Garty, H., and B. Lindemann. 1984. Feedback inhibition of sodium uptake in K^+-depolarized toad urinary bladder. *Biochim. Biophys. Acta.* 771:89–98.

Garty, H., and C. Asher. 1985. Ca dependent, temperature sensitive, regulation of Na channels in tight epithelia. A study using membrane vesicles. *J. Biol. Chem.* 260:8330–8335.

Garty, H., and C. Asher. 1986. Ca^{2+} induced down regulation of Na^+ channels in toad bladder epithelium. *J. Biol. Chem.* 261: 7400–7406.

Garty, H., and L.G. Palmer. 1997. Epithelial sodium channels: function, structure, and regulation. *Physiol. Rev.* 77:359–396.

Garty, H., C. Asher, and O. Yeger. 1987. Direct inhibition of epithelial Na^+ channels by a pH dependent interaction with calcium, and by other divalent ions. *J. Membr. Biol.* 95:151–162.

Goldstein, O., C. Asher, and H. Garty. 1997. Cloning and induction by low NaCl intake of avian intestine Na channel subunits. *Am. J. Physiol.* 272:C270–C277.

Hamill, O.P., A. Marty, E. Neher, B. Sakmann, and F.S. Sigworth. 1981. Improved patch-clamp techniques for high resolution current recording from cells and cell free membrane patches. *Pflügers Arch.* 391:85–100.

Hirt, R., O. Poulain-Godefroy, J. Billotte, J.-P. Kraehenbuhl, and N.

Fasel. 1992. Highly inducible synthesis of heterologous proteins in epithelial cells carrying a glucocorticoid responsive vector. *Gene.* 111:199–206.

Hummler, E., P. Barker, J. Gatzy, F. Beermann, C. Verdumo, A. Schmidt, R.C. Boucher, and B.C. Rossier. 1996. Early death due to defective neonatal lung liquid clearance in αENaC-deficient mice. *Nat. Genet.* 12:325–328.

Ismailov, I.I., B.K. Berdiev, and D.J. Benos. 1995. Regulation by Na^+ and Ca^{2+} of renal epithelial Na channels reconstituted into planar lipid bilayers. *J. Gen. Physiol.* 106:445–466.

Ismailov, I.I., M.S. Awayda, B.K. Berdiev, J.K. Bubien, J.E. Lucas, C.M. Fuller, and D.J. Benos. 1996. Triple-barrel organization of ENaC, a cloned epithelial Na^+ channel. *J. Biol. Chem.* 271:807–816.

Ismailov, I.I., B.K. Berdiev, V.G. Shlyonsky, C.M. Fuller, A.G. Prat, B. Jovov, H.F. Cantiello, D.A. Ausiello, and D.J. Benos. 1997. Role of actin in regulation of epithelial sodium channels by CFTR. *Am. J. Physiol.* 272:C1077–C1086.

Komwatana, P., A. Dinudom, J.A. Young, and D.I. Cook. 1996*a*. Control of the amiloride-sensitive Na^+ current in salivary duct cells by extracellular sodium. *J. Membr. Biol.* 150:133–141.

Komwatana, P., A. Dinudom, J.A. Young, and D.I. Cook. 1996*b*. Cytosolic Na^+ controls an epithelial Na^+ channel via the Go guanine nucleotide-binding regulatory protein. *Proc. Natl. Acad. Sci. USA.* 93:8107–8111.

Lang, F., F. Friedrich, M. Paulmichl, W. Schobersberger, A. Jungwirth, M. Ritter, M. Steidl, H. Weiss, E. Wöll, E. Tschernko, R. Paulmichl, and C. Hallbrucker. 1990. Ion channels in Madin-Darby Canine Kidney cells. *Renal Physiol. Biochem.* 13:82–93.

Li, J.H.-Y., L.G. Palmer, I.S. Edelman, and B. Lindemann. 1982. The role of the sodium channel density in the natriferic response of the toad urinary bladder to an antidiuretic hormone. *J. Membr. Biol.* 64:79–89.

Ling, B.N., and D.C. Eaton. 1989. Effects of luminal Na^+ on single Na^+ channels in A6 cells: a regulatory role for protein kinase C. *Am. J. Physiol.* 256:F1094–F1103.

Lingueglia, E., N. Voilley, R. Waldmann, M. Lazdunski, and P. Barbry. 1993. Expression cloning of an epithelial amiloride-sensitive Na^+ channel. A new channel type with homologies to *Caenorhabditis elegans* degenerins. *FEBS Lett.* 318:95–99.

Lingueglia, E., S. Renard, R. Waldmann, N. Voilley, G. Champigny, H. Plass, M. Lazdunski, and P. Barbry. 1994. Different homologous subunits of the amiloride-sensitive Na^+ channel are differently regulated by aldosterone. *J. Biol. Chem.* 269:13736–13739.

McDonald, F.J., P.M. Snyder, P.B. McCray, and M.J. Welsh. 1994. Cloning, expression, and distribution of a human amiloride-sensitive Na^+ channel. *Am. J. Physiol.* 266:L728–L734.

McDonald, F.J., M.P. Price, P.M. Snyder, and M.J. Welsh. 1995. Cloning and expression of the β- and γ-subunits of the human epithelial sodium channel. *Am. J. Physiol.* 268:C1157–C1163.

McNicholas, C.M., and C.M. Canessa. 1997. Diversity of channels generated by different combinations of epithelial sodium channel subunits. *J. Gen. Physiol.* 109:681–692.

Oiki, S., and Y. Okada. 1987. Ca-EGTA buffer in physiological solutions. *Seitai-no-kagaku.* 38:79–83.

Palmer, L.G. 1985. Modulation of apical Na permeability of the toad urinary bladder by intracellular Na, Ca, and H. *J. Membr. Biol.* 83:57–69.

Palmer, L.G. 1992. Epithelial Na channels: function and diversity. *Annu. Rev. Physiol.* 54:51–66.

Palmer, L.G., and G. Frindt. 1986. Amiloride-sensitive Na channels from the apical membrane of the rat cortical collecting tubule. *Proc. Natl. Acad. Sci. USA.* 83:2767–2770.

Palmer, L.G., and G. Frindt. 1987. Effects of cell Ca and pH on Na channels from rat cortical collecting tubules. *Am. J. Physiol.* 253: F333–F339.

Palmer, L.G., and G. Frindt. 1988. Conductance and gating of epithelial Na channels from rat cortical collecting tubule. Effects of luminal Na and Li. *J. Gen. Physiol.* 92:121–138.

Palmer, L.G., and G. Frindt. 1996. Gating of Na channels in the rat cortical collecting tubule: effects of voltage and membrane stretch. *J. Gen. Physiol.* 107:35–45.

Palmer, L.G., I.S. Edelman, and B. Lindemann. 1980. Current–voltage analysis of apical sodium transport in toad urinary bladder: effects of inhibitors of transport and metabolism. *J. Membr. Biol.* 57: 59–71.

Palmer, L.G., G. Frindt, R.B. Silver, and J. Strieter. 1989. Feed-back regulation of epithelial sodium channels. *Curr. Top. Membr. Transp.* 34:45–60.

Plant, P., H. Yeger, O. Staub, P. Howard, and D. Rotin. 1997. The C2 Domain of the ubiquitin protein ligase Nedd4 mediates Ca^{2+}-dependent plasma membrane localization. *J. Biol. Chem.* 272: 32329–32336.

Puoti, A., A. May, C.M. Canessa, J.-D. Horisberger, L. Schild, and B.C. Rossier. 1995. The highly selective low-conductance epithelial Na^+ channel of *Xenopus laevis* A6 kidney cells. *Am. J. Physiol.* 38:C188–C197.

Renard, S., E. Lingueglia, N. Voilley, M. Lazdunski, and P. Barbry. 1994. Biochemical analysis of the membrane topology of the amiloride-sensitive Na^+ channel. *J. Biol. Chem.* 269:12981–12986.

Rossier, B.C., and L.G. Palmer. 1992. Mechanisms of aldosterone action on sodium and potassium transport. *In* The Kidney: Physiology and Pathophysiology. D.W. Seldin and G. Giebisch, editors. Raven Press, New York. 1373–1409.

Schild, L., E. Schneeberger, I. Gautschi, and D. Firsov. 1997. Identification of amino acid residues in the alpha, beta and gamma subunits of the epithelial sodium channel (ENaC) involved in amiloride block and ion permeation. *J. Gen. Physiol.* 109:15–26.

Shimkets, R.A., D.G. Warnock, C.M. Bositis, C. Nelson-Williams, J.H. Hansson, M. Schambelan, J.R. Gill, S. Ulick, R.V. Milora, J.W. Findling, et al. 1994. Liddle's syndrome: heritable human hypertension caused by mutations in the β subunit of the epithelial sodium channel. *Cell.* 79:407–414.

Silver, R.B., G. Frindt, E.E. Windhager, and L. Palmer. 1993. Feedback regulation of Na channels in rat CCT. I. Effect of inhibition of Na pump. *Am. J. Physiol.* 264:F557–F564.

Snyder, P.M., F.J. McDonald, J.B. Stokes, and M.J. Welsh. 1994. Membrane topology of the amiloride-sensitive epithelial sodium channel. *J. Biol. Chem.* 269:24379–24383.

Staub, O., S. Dho, P.C. Henry, J. Correa, T. Ishikawa, J. McGlade, and D. Rotin. 1996. WW domains of Nedd4 bind to the proline-rich PY motifs in the epithelial Na^+ channel deleted in Liddle's syndrome. *EMBO (Eur. Mol. Biol. Organ.) J.* 15:2371–2380.

Staub, O., I. Gautschi, T. Ishikawa, K. Breitschopf, A. Ciechanover, L. Schild, and D. Rotin. 1997. Regulation of stability and function of the epithelial Na^+ channel (ENaC) by ubiquitination. *EMBO (Eur. Mol. Biol. Organ.) J.* 16:6325–6336.

Strautnieks, S.S., R.J. Thompson, R.M. Gardiner, and E. Chung. 1996. A novel splice-site mutation in the gamma subunit of the epithelial sodium channel gene in three pseudohypoaldosteronism type 1 families. *Nat. Genet.* 13:248–250.

Stühmer, W. 1992. Electrophysiological recording from *Xenopus* oocytes. *Methods Enzymol.* 207:319–339.

Stutts, M.J., C.M. Canessa, J.C. Olsen, M. Hamrick, J.A. Cohn, B.C. Rossier, and R.C. Boucher. 1995. CFTR as a cAMP-dependent regulator of sodium channels. *Science.* 269:847–850.

Stutts, M.J., B.C. Rossier, and R.C. Boucher. 1997. CFTR inverts PKA-mediated regulation of ENaC. *J. Biol. Chem.* 272:14037–14040.

Thompson, S.M., and J.H. Sellin. 1986. Relationships among sodium current, permeability, and sodium activities in control and glucocorticoid-stimulated rabbit descending colon. *J. Membr. Biol.* 92:121–134.

Turnheim, K., S.M. Thompson, and S.G. Schultz. 1983. Relation between intracellular sodium active transport in rabbit colon: current–voltage relations of the apical sodium entry mechanism in the presence of varying luminal sodium concentrations. *J. Membr. Biol.* 76:299–309.

Voilley, N., E. Lingueglia, G. Champigny, M.-G. Mattéi, R. Waldmann, M. Lazdunski, and P. Barbry. 1994. The lung amiloride-sensitive Na^+ channel: biophysical properties, pharmacology, ontogenesis, and molecular cloning. *Proc. Natl. Acad. Sci. USA.* 91:247–251.

Warncke, J., and B. Lindemann. 1985. Voltage dependence of Na^+ channel blockage by amiloride: relaxation effects in admittance spectra. *J. Membr. Biol.* 86:255–265.

Woodhull, A. 1973. Ionic blockage of sodium channels in nerve. *J. Gen. Physiol.* 61:687–708.